

Characterizing the Atmospheric Mn Cycle and Its Impact on Terrestrial Biogeochemistry

Louis Lu¹, Longlei Li², Sagar Dilipbhai Rathod³, Peter George Hess², Carmen Enid Martinez², Nicole M Fernandez², Christine Goodale², Janice E. Thies², Michelle Y Wong⁴, Maria Grazia Alaimo⁵, Paulo Artaxo⁶, Francisco Barraza⁷, África Barreto⁸, David C.S. Beddows⁹, Shankar Chellam¹⁰, Ying Chen¹¹, Patrick Y. Chuang¹², David Damien Cohen¹³, Gaetano Dongarra⁵, Cassandra J. Gaston¹⁴, Dario Gomez¹⁵, Yasser Morera-Gomez¹⁶, Hannele Hakola¹⁷, Jenny L Hand¹⁸, Roy M. Harrison⁹, Philip K. Hopke¹⁹, Christoph Hueglin²⁰, Yuan-wen Kuang²¹, Katriina Kyllönen²², Fabrice Lambert²³, Willy Maenhaut²⁴, Randall V Martin²⁵, Adina Paytan²⁶, Joseph M. Prospero¹⁴, Yenny González²⁷, Sergio Rodriguez²⁸, Patricia Smichowski¹⁵, Daniela Varrica⁵, Brenna Walsh²⁵, Crystal Weagle²⁵, Yi-hua Xiao²⁹, and Natalie M Mahowald²

¹Duke University

²Cornell University

³La Follette School of Public Affairs, University of Wisconsin

⁴Cary Institute of Ecosystem Studies

⁵University of Palermo

⁶University of Sao Paulo

⁷Saw Science

⁸AEMET

⁹University of Birmingham

¹⁰Texas A&M University

¹¹Fudan University

¹²UC Santa Cruz

¹³ANSTO

¹⁴University of Miami

¹⁵Comisión Nacional de Energía Atómica

¹⁶Universidad de Navarra

¹⁷Finnish meteorological institute

¹⁸Colorado State University

¹⁹University of Rochester

²⁰EMPA

²¹South China Botanical Garden

²²Finnish Meteorological Institute

²³Pontifical Catholic University of Chile

²⁴Ghent University

²⁵Washington University in St. Louis

²⁶UCSC

²⁷CIMEL Electronique

²⁸CSIC - Spanish National Research Council

²⁹Research Institute of Tropical Forestry, Chinese Academy of Forestry

September 11, 2023

Abstract

Manganese (Mn) is a key cofactor in enzymes responsible for lignin decay (mainly Mn peroxidase), regulating the rate of litter degradation and carbon (C) turnover in temperate and boreal forest biomes. While soil Mn is mainly derived from bedrock, atmospheric Mn could also contribute to soil Mn cycling, especially within the surficial horizon, with implications for soil C cycling. However, quantification of the atmospheric Mn cycle, which comprises emissions from natural (desert dust, sea salts, volcanoes, primary biogenic particles, and wildfires) and anthropogenic sources (e.g. industrialization and land-use change due to agriculture) transport, and deposition into the terrestrial and marine ecosystem, remains uncertain. Here, we use compiled emission datasets for each identified source to model and quantify the atmospheric Mn cycle with observational constraints. We estimated global emissions of atmospheric Mn in aerosols ($<10 \mu\text{m}$ in aerodynamic diameter) to be 1500 Gg Mn yr⁻¹. Approximately 32% of the emissions come from anthropogenic sources. Deposition of the anthropogenic Mn shortened soil Mn “pseudo” turnover times in surficial soils about 1-m depth (ranging from 1,000 to over 10,000,000 years) by 1-2 orders of magnitude in industrialized regions. Such anthropogenic Mn inputs boosted the Mn-to-N ratio of the atmospheric deposition in non-desert dominated regions (between 5×10^{-5} and 0.02) across industrialized areas, but still lower than soil Mn-to-N ratio by 1-3 orders of magnitude. Correlation analysis revealed a negative relationship between Mn deposition and topsoil C density across temperate and (sub)tropical forests, illuminating the role of Mn deposition in these ecosystems.

Hosted file

973441_0_art_file_11362392_s0nb47.docx available at <https://authorea.com/users/661368/articles/664495-characterizing-the-atmospheric-mn-cycle-and-its-impact-on-terrestrial-biogeochimistry>

Hosted file

973441_0_supp_11362393_s0nb47.docx available at <https://authorea.com/users/661368/articles/664495-characterizing-the-atmospheric-mn-cycle-and-its-impact-on-terrestrial-biogeochimistry>

1

2 **Characterizing the Atmospheric Mn Cycle and Its Impact on Terrestrial** 3 **Biogeochemistry**

4 **Louis Lu^{1,2}, Longlei Li¹, Sagar Rathod³, Peter Hess⁴, Carmen Martínez⁵, Nicole**
 5 **Fernandez¹, Christine Goodale⁶, Janice Thies⁵, Michelle Wong⁷, Maria Alaimo¹⁶, Paulo**
 6 **Artaxo⁸, Francisco Barraza⁹, Africa Barreto¹⁰, David Beddows¹¹, Shankarararman**
 7 **Chellam¹², Ying Chen¹³, Patrick Chuang¹⁴, David Cohen¹⁵, Gaetano Dongarrà¹⁶,**
 8 **Cassandra Gaston¹⁷, Darío Gómez¹⁸, Yasser Morera-Gómez¹⁹, Hannele Hakola²⁰, Jenny**
 9 **Hand²¹, Roy Harrison^{11,22}, Phillip Hopke²³, Christoph Hueglin²⁴, Yuan-wen Kuang²⁵,**
 10 **Katriina Kyllonen²⁰, Fabrice Lambert^{26,27}, Willy Maenhaut²⁸, Randall Martin²⁹, Adina**
 11 **Paytan¹³, Joseph Prospero¹⁷, Yenny González^{10,30}, Sergio Rodriguez^{10,31}, Patricia**
 12 **Smichowski¹⁸, Daniela Varrica¹⁶, Brenna Walsh²⁹, Crystal Weagle²⁹, Yi-hua Xiao²⁴, and**
 13 **Natalie Mahowald¹**

14 ¹Department of Earth and Atmospheric Sciences, Cornell University, Ithaca, NY, USA, ²Now at:
 15 Nicholas School of the Environment, Duke University, Durham, NC, USA, ³La Follette School
 16 of Public Affairs, University of Wisconsin, WI, Madison, USA, ⁴Biological and Environmental
 17 Engineering, Cornell University, Ithaca, NY, USA, ⁵School of Integrative Plant Sciences,
 18 Cornell University, Ithaca, NY, USA, ⁶Department of Ecology and Evolutionary Biology,
 19 Cornell University, Ithaca, NY, USA, ⁷Department of Ecology and Evolutionary Biology, Yale
 20 University, New Haven, CT 065118, ⁸Instituto de Fisica, Universidade de Sao Paulo, 05508-090,
 21 Sao Paulo, SP, Brazil, ⁹Saw Science, Invercargill, New Zealand, ¹⁰Izana Atmospheric Research
 22 Centre AEMET, Joint Research Unit to CSIC “Climate and Composition of the Atmosphere”, La
 23 Marina 20, planta 6,38001, Santa Cruz de Tenerife, Spain, ¹¹School of Geography, Earth and
 24 Environmental Sciences, University of Birmingham, Edgbaston, Birmingham B15 2TT, United
 25 Kingdom, ¹²Department of Civil & Environmental Engineering, Texas A&M University, College
 26 Station, TX 77843-3136, USA, ¹³Institute of Marine Sciences, University of California, Santa
 27 Cruz, CA, USA, ¹⁴Earth & Planetary Sciences Department, University of California, Santa Cruz,
 28 CA, 95064, USA, ¹⁵Australian Nuclear Science and Technology Organisation, Lucas Heights,
 29 NSW, Australia, ¹⁶Dip. Scienze della Terra e del Mare, University of Palermo, Italy, ¹⁷Rosenstiel
 30 School of Marine and Atmospheric Science, University of Miami, Miami, FL, 33149, USA,
 31 ¹⁸Comisión Nacional de Energía Atómica, Universidad de Buenos Aires, Argentina, ¹⁹
 32 Universidad de Navarra, Instituto de Biodiversidad y Medioambiente BIOMA, Irunlarrea 1,
 33 31008, Pamplona, España, ²⁰Finnish Meteorological Institute, Helsinki, Finland, ²¹Cooperative
 34 Institute for Research in the Atmosphere, Colorado State University, Fort Collins, CO, USA,
 35 ²²Department of Environmental Sciences, Faculty of Meteorology, Environment and Arid Land
 36 Agriculture, King Abdulaziz University, Jeddah, Saudi Arabia, ²³Department of Chemical and
 37 Biomolecular Engineering, Clarkson University, Potsdam, NY, USA, ²⁴Swiss Federal
 38 Laboratories for Materials Science and Technology (EMPA), CH-8600 Duebendorf,
 39 Switzerland, ²⁵Key Laboratory of Vegetation Restoration and Management of Degraded
 40 Ecosystems, South China Botanical Garden, Chinese Academy of Sciences, Guangzhou 510650,
 41 China, ²⁶Geography Institute, Pontificia Universidad Católica de Chile, Santiago, 7820436,
 42 Chile, ²⁷Center for Climate and Resilience Research, University of Chile, Santiago, Chile,
 43 ²⁸Department of Chemistry, Ghent University, Gent, Belgium, Institute for Nuclear Sciences,

44 University of Gent, Belgium, ²⁹Energy, Environmental and Chemical Engineering, Washington
45 University, St. Louis, MO, USA, ³⁰CIMEL Electronique, Paris, 75011, France, ³¹Instituto de
46 Productos Naturales y Agrobiología IPNA CSIC, La Laguna, Canary Islands, Spain.

47 Corresponding author: Louis Lu (pl230@duke.edu)

48 †Additional author notes should be indicated with symbols (current addresses, for example).

49 **Key Points:**

- 50 • We modelled the atmospheric manganese (Mn) cycle from emission to deposition and
51 compared our aerosol model to existing observations based on our compilation.
- 52 • Anthropogenic activity contributes to approximately one-third of global atmospheric Mn,
53 shortening the soil Mn turnover time by 1 to 2 orders of magnitude.
- 54 • Mn correlates with topsoil carbon (C) in temperate and (sub)tropical forests, along with N
55 deposition and other climatic factors.

56 **Abstract**

57 Manganese (Mn) is a key cofactor in enzymes responsible for lignin decay (mainly Mn
58 peroxidase), regulating the rate of litter degradation and carbon (C) turnover in temperate and
59 boreal forest biomes. While soil Mn is mainly derived from bedrock, atmospheric Mn could also
60 contribute to soil Mn cycling, especially within the surficial horizon, with implications for soil C
61 cycling. However, quantification of the atmospheric Mn cycle, which comprises emissions from
62 natural (desert dust, sea salts, volcanoes, primary biogenic particles, and wildfires) and
63 anthropogenic sources (e.g. industrialization and land-use change due to agriculture) transport,
64 and deposition into the terrestrial and marine ecosystem, remains uncertain. Here, we use
65 compiled emission datasets for each identified source to model and quantify the atmospheric Mn
66 cycle with observational constraints. We estimated global emissions of atmospheric Mn in
67 aerosols ($<10\ \mu\text{m}$ in aerodynamic diameter) to be $1500\ \text{Gg Mn yr}^{-1}$. Approximately 32% of the
68 emissions come from anthropogenic sources. Deposition of the anthropogenic Mn shortened soil
69 Mn “pseudo” turnover times in surficial soils about 1-m depth (ranging from 1,000 to over
70 10,000,000 years) by 1-2 orders of magnitude in industrialized regions. Such anthropogenic Mn
71 inputs boosted the Mn-to-N ratio of the atmospheric deposition in non-desert dominated regions
72 (between 5×10^{-5} and 0.02) across industrialized areas, but still lower than soil Mn-to-N ratio by
73 1-3 orders of magnitude. Correlation analysis revealed a negative relationship between Mn
74 deposition and topsoil C density across temperate and (sub)tropical forests, illuminating the role
75 of Mn deposition in these ecosystems.

76 **1 Introduction**

77 As an essential trace element and micronutrient, manganese (Mn) has been identified to be
78 closely related to soil carbon (C) turnover because of its role of regulating soil organic matter
79 (SOM) decomposition by enhancing the activity of lignin-decay enzymes (mainly Mn
80 peroxidase, MnP) and hence the oxidative decomposition of lignin (Berg et al., 2007; Hofrichter,
81 2002). Mn limitation and the associated fungal community change from N deposition have been
82 proposed as an explanation for the suppressing effect of long-term atmospheric nitrogen (N)
83 deposition on SOM decomposition (Moore et al., 2021; Whalen et al., 2018).

84
85 Studies have assessed the relationship between Mn and soil C turnover using various indicators
86 including Mn concentration in litter, rate or extent of decomposition of litter (Berg et al., 2007,
87 2010; Berg 2000; Davey et al., 2007; Trum et al., 2015), soil Mn and total C concentrations
88 (Stendahl et al., 2017), MnP enzymatic activity, and fungal community structures (Kranabetter et
89 al., 2021; Moore et al., 2021; Whalen et al., 2018). However, no previous study has examined the
90 impact of atmospheric Mn deposition on soil C turnover, nor has such a relationship been
91 quantified on a global scale. In fact, atmospheric deposition has been identified as a major source
92 of metal(loid) accumulation, including Mn, in surficial soil layers (He & Walling, 1997; Kaste et
93 al., 2003; Puchelt et al., 1993; Wang et al., 2022) where most fresh organic matter accumulates,
94 underlining the need to characterize atmospheric Mn deposition for more advanced
95 understanding of soil C turnover.

96
97 While atmospheric Mn deposition has not been extensively investigated, studies have shown the
98 importance of atmospheric deposition of iron (Fe), which has similar biogeochemical properties
99 as Mn (Canfield et al., 2005), for understanding marine biogeochemistry (Mahowald et al.,
100 2009). In oceans, atmospheric deposition of Fe could be a stronger source of Fe than the

101 weathering of rock (Canfield et al., 2005); Mn deposition could act similarly as a non-negligible
102 source of ocean Mn which could have significant ecological relevance such as co-limitation of
103 phytoplankton growth with Fe (Browning et al., 2021; Mahowald et al., 2018). More recently,
104 Mn catalysis of organic C polymerization reactions was proposed to result in organic carbon
105 preservation and storage in marine sediments (Moore et al., 2023). Together, these studies show
106 that atmospheric Mn deposition could play an important role in the global Mn cycle and is likely
107 linked to functions carried out by Mn in both terrestrial and marine ecosystems.

108
109 There is a variety of natural sources of Mn, such as desert dust (the single dominant source), sea
110 salts, volcanoes, wildfires, and primary biogenic particles (Nriagu, 1989; Pacyna & Pacyna,
111 2001). In addition to natural sources of atmospheric Mn deposition, humans can perturb the
112 global atmospheric Mn cycle by significantly altering desert dust and adding anthropogenic
113 emission sources, such as combustion (Mahowald et al., 2018). Anthropogenic aerosols have the
114 potential to inducing a more rapid impact on ecosystems because of their higher solubility owing
115 to their smaller particle size, higher carbon content, chemical and surface associations, and
116 reactions that occur during the process of combustion (Desboeufs et al., 2005; Jang et al., 2007;
117 Sedwick et al., 2007; Voutsas & Samara, 2002) compared to natural aerosols.

118
119 While global budgets for many metals have been estimated previously, the spatial distribution of
120 Mn deposition and the overlap with N deposition are unknown. Nriagu (1989) made the first
121 attempt to estimate Mn emissions to the atmosphere. Nriagu (1989) and Pacyna & Pacyna (2001)
122 identified desert dust as the single dominant source, and estimated the contribution of
123 anthropogenic sources to be approximately 11%. Mahowald et al. (2018) estimated that
124 anthropogenic emissions represented ~1% of the total aerosol Mn sources. Uncertainties are high
125 due to the lack of observational data, and so far, there have been no detailed spatially explicit
126 studies of the atmospheric Mn cycle. Therefore, a better estimation of the Mn source budget
127 (both natural and anthropogenic) along with its spatial distribution is necessary for understanding
128 the global Mn cycle and its influence on terrestrial ecosystems.

129
130 In this study, we conducted the first 3-d modeling of the emission, atmospheric transport, and
131 deposition of atmospheric Mn from multiple sources including natural and anthropogenic dust,
132 sea salts, volcanoes, wildfires, and primary biogenic particles. We compile emission datasets for
133 each source and soil Mn concentration measurements for the emission modeling and model
134 calibration, respectively. We synthesized observational and modeling evidence to characterize
135 the spatial distribution of atmospheric Mn and to assess the anthropogenic perturbation to it in
136 both PM_{2.5} and PM₁₀ size fractions (atmospheric particulate matter, PM, <2.5 and 10 μm in
137 aerodynamic diameter, respectively), which are used as common measures for aerosols in the
138 atmosphere and included in the model (Mahowald et al., 2014; Ryder et al., 2019). To
139 understand the importance of atmospheric deposition as a flux in the Mn cycle and as a source of
140 Mn addition to soils in terrestrial ecosystems, we interpreted soil Mn “pseudo” turnover times
141 and Mn-to-N ratios in deposition as well as the relationship between Mn deposition and C
142 density in topsoil.
143

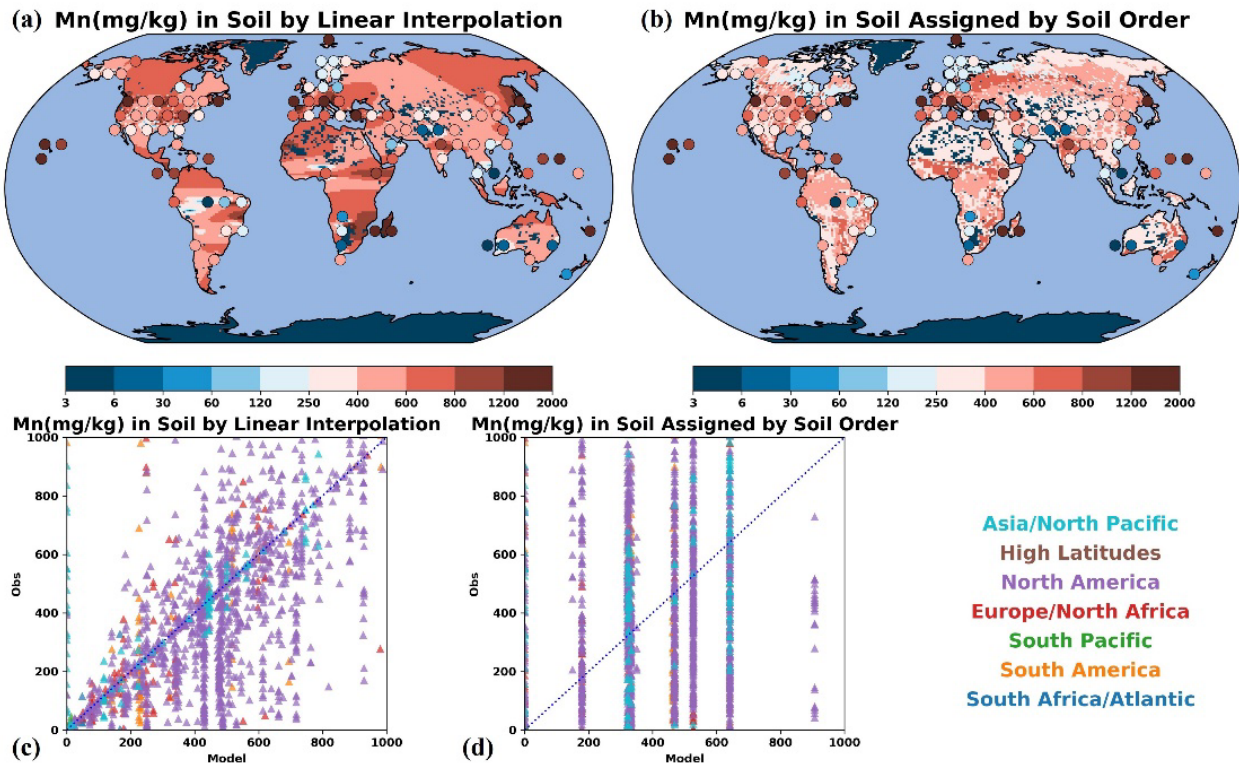
144 **2 Materials and Methods**

145 2.1 Soil Mn Observations and Interpolation

146 We compiled soil observational data collected from 94 studies found using the Thomson Web of
147 Science Core Collection on March 20, 2022 and the soil characterization database provided in
148 National Cooperative Soil Survey (NCSS). There are 2068 individual data points in total,
149 reporting worldwide Mn concentrations in surface soils based on several extraction and digestion
150 methods (Data Set S1). A standard approach is HNO₃ + HCl acid digestion as outlined by the
151 U.S. Department of Agriculture (USDA) and Natural Resources Conservation Service (NRCS)
152 (Soil Survey Staff, 2011). If detailed geographical coordinates were not explicitly provided, we
153 assigned the observation of the nearest latitude and longitude based on available information
154 about its location. Two approaches (linear interpolation and extrapolation by soil type) were used
155 to extrapolate the limited observational data to provide global estimates of Mn distributions in
156 soils.

157 2.1.1 Linear Interpolation

158 Our first approach was to linearly interpolate observed soil Mn concentrations according to their
159 geographical coordinates and extrapolate them on a global map (Figure 1a) using inverse
160 distance method in GRIDDATA function on board with Interactive Data Language. Because
161 directly extrapolating all available soil Mn data is a straightforward, the constructed soil map
162 from linear interpolation was a fairly good representation of observations ($r = 0.66$; Figure 1a).
163 Nonetheless, the correlation was weaker than one would expect for linear interpolation due to the
164 model grid resolution and the fact that many observational sites clustered in a single grid.
165 Because ice and glaciers were not considered as soil, and available observations near the poles
166 were lacking, Mn concentrations in glaciated areas (mostly Greenland and Antarctica) were
167 masked and assigned a minimum value.



168

169

170

171

172

173

174

175

176

177

178

179

180

181

182

183

184

185

186

187

188

189

190

Figure 1. (a) Map of estimated global soil Mn concentration constructed from linear interpolation and (b) by soil-order extrapolation. The base map is compared to 2068 individual observational points (mg kg⁻¹ Mn in surface soils), which are spatially averaged and plotted as circles filled with colors corresponding to their Mn concentration (Abanda et al., 2011; Alfaro et al., 2015; Alongi et al., 2004; Andruszczak E., 1975; Asawalam & Johnson, 2007; Becquer et al., 2010; Beygi & Jalali, 2018; Bibak et al., 1994; Boente et al., 2017; Bradford et al., 1996; Buccolieri et al., 2010; Burt et al., 2011; Cabrera et al., 1999; Cancela et al., 2002; Cassol et al., 2020; Chen et al., 1991; Chen et al., 1999, 2000; da Silva Costa et al., 2017; da Silva et al., 2015; Dantu, 2010a, 2010b; Darwish & Poellmann, 2015; de Souza et al., 2015; do Nascimento et al., 2018; Dolan et al., 1990; Fernandes et al., 2018; Foulds, 1993; Franklin et al., 2003; Ghaemi et al., 2015; Haynes & Swift, 1991; Hsu et al., 2016; Hua et al., 2013; Ikem et al., 2008; Imran et al., 2010; Iñigo et al., 2011; Ivezic et al., 2011; Jahiruddin et al., 2000; Joshi et al., 2017; Kassaye et al., 2012; Kloss et al., 2014; Lavado & Porcelli, 2000; Lindell et al., 2010; Ma et al., 1997; Mashi et al., 2004; McKenzie, 1957; Michopoulos et al., 2004, 2017; Mikkonen et al., 2017; Miko et al., 2003; Morales Del Mastro et al., 2015; Nalovic & Pinta, 1969; Nanzyo et al., 2002; Natali et al., 2009; Navas & Lindhorfer, 2005; Nguyen et al., 2018; Njofang et al., 2009; Nygard et al., 2012; Papadopoulos et al., 2009; Papastergios et al., 2011; Patel et al., 2015; Paye et al., 2010; Preda & Cox, 2002; Rashed, 2010; Rekasi & Filep, 2012; Richards et al., 2012; Roca et al., 2012; Roca-Perez et al., 2004, 2010; Rusjan et al., 2006; Saglam, 2017; Sako et al., 2009; Salonen & Korkka-Niemi, 2007; Sheikh-Abdullah, 2019; Sheppard et al., 2009; Skordas et al., 2013; Smeltzer et al., 1962; Stajković-Srbinić et al., 2018; Stankovic et al., 2012; Stehouwer et al., 2010; Steinnes et al., 2000; Sterckeman et al., 2006a; Sterckeman et al., 2006b;

191 Su & Yang, 2008; Tsikritzis et al., 2002; Tume et al., 2011; Tyler, 2004; Vance & Entry, 2000;
192 Vojnovic et al., 2018; Wen et al., 2018; Wilcke et al., 2005; Xianmo et al., 1983; Yalcin et al.,
193 2007; Yang et al., 2012; Yang et al., 2013; Yilmaz et al., 2003; Yu et al., 2012; Zhang et al.,
194 2009; Zorer et al., 2009). (c) Scatter plot showing how well the linearly interpolated map
195 represents the observations ($n = 2068$, $r = 0.66$). (d) Same as (c), except for targeting the soil-
196 order extrapolated map. Model values equal observational values along the blue dotted diagonal
197 ($n = 2068$, $r = 0.08$). Colors indicate the locations of studies listed in the legend. Citations of
198 each study and details on its extraction/digestion methods are included in the supporting
199 information (Data Set S1).

200

201 2.1.2 Extrapolation by Soil Type

202 In our second approach, we categorized Mn concentration observations according to their soil
203 taxonomic classification. Using the same method as in Wong et al. (2021), we processed Mn
204 concentration from 1574 (out of 2068) data points which provided in-situ soil classification
205 information in either the United States Department of Agriculture (USDA), Food and
206 Agriculture (FAO) taxonomic system, or the World Reference Base for Soil Resources (WRB)
207 (the latter two were converted into USDA classification). A median value was assigned for each
208 of the 12 USDA soil orders and the Mn concentration was extrapolated to the $1^\circ \times 1^\circ$ USDA-
209 NRCS Global Soil Regions map based on a reclassification of the FAO-UNESCO Soil Map of
210 the World (Figure 1b) (Batjes, 1997). In addition to the 12 soil orders, the map also identified
211 lands that were not covered by soils, including ice/glaciers, moving sands, rocky terrains, and
212 water bodies, whose Mn concentration was masked and set to the minimum.

213

214 Nonetheless, because the Mn variability within soil orders were shown to be on the same level as
215 that between soil orders (Figure S1), Mn concentration might not be well-distinguished in
216 different soil orders. In addition, the number of available soil measurements varied greatly
217 between different orders (Table S1) so that in cases where very few observations existed (e.g.
218 gelisol), the median value of the soil Mn concentration would be much less representative. Our
219 soil data inventory reflected the heterogeneous nature of the spatial distribution of the soil and its
220 Mn content, which could not be well-represented by soil-type extrapolation. Overall, the soil-
221 order based map did not compare as well to the in-situ soil Mn observations as the linear
222 interpolation (Figure 1d). Therefore, the soil map and model simulations constructed using linear
223 interpolation were primarily considered in data analysis and interpretation, with results obtained
224 by soil-type extrapolation listed in supplementary materials and minorly concerned. Given the
225 scarce nature of soil Mn observations, we kept the soil-type extrapolation method, as it might
226 still be a reasonable approach to estimate and constrain soil Mn values, especially in regions
227 lacking direct observations, such as the higher latitudes.

228

229 2.2 Atmospheric Modeling

230 We simulated global atmospheric Mn emissions, transport, and deposition using the Community
231 Atmosphere Model, version 6 (CAM6), the atmospheric component of the Community Earth
232 System Model (version 2; CESM2) developed at the National Center for Atmospheric Research
233 (NCAR) (Hurrell et al., 2013; Liu et al., 2011), with the four-mode (Aitken, accumulation,
234 coarse, and primary) modal aerosol model (MAM4) (Liu et al., 2016). Three out of the four
235 modes contain dust aerosols which are modeled as eight different types of dust mineral
236 components (Liu et al., 2011; Scanza et al., 2015; Hamilton et al., 2019; Li et al., 2021, 2022).
237 Model simulations were conducted for four years, with the last three years (2013-2015) used for
238 analysis (Computational and Information Systems Laboratory, 2019). We nudged the model
239 toward MERRA2 meteorology fields (Gelaro et al., 2017).

240
241 The model simulates three-dimensional transport and wet and dry deposition for gases and
242 particles which are internally/externally mixed within/between the modes. The dry deposition
243 parameterization follows Petroff and Zhang (2010) as previously implemented in CAM6 (Li et
244 al., 2022 ; see descriptions therein for the wet deposition scheme as well). We modified the
245 model to allow for the advection of Mn from different sources. Both natural and anthropogenic
246 sources were determined to possess large uncertainties in strength. We used a first estimate
247 assuming that the full uncertainty range is one order of magnitude. Therefore, we included a
248 range of values (typically a factor of 10) for the Mn contribution from each source (Table 1). To
249 better fit the observational data, we “tuned” the model making a particular effort to adjust
250 anthropogenic emissions both because of their larger uncertainties compared to natural emissions
251 and because the largest discrepancies occurred over industrialized regions (see below). The
252 choice of the “tuning” for each source was done using a trial-and-error method using
253 observational evidence. In addition, we report our best estimates and assume a large uncertainty:
254 in most cases at least one order of magnitude because of the limited data as previous studies
255 suggest (e.g. Nriagu, 1989; Mahowald et al., 2018).

256

257 Table 1

258 *Mn Emission Factor (composition) in Sources and Atmospheric Mn Budgets Based on*
259 *Simulations from the Community Atmosphere Model (CAM) (v6)*

260

Source	Mn composition	Composition citation	Global source Mn (Gg yr ⁻¹) [ranges] (% fine)	Global source Mn (Gg yr ⁻¹) from reference*
Desert dust	0.1-5479 mg kg ⁻¹	This study	950 [290-4800] (1.7)	42-400 ^a 900 ^b
Agricultural dust	0.1-5479 mg kg ⁻¹	This study	390 [120-1900] (1.7)	
Sea-salt aerosols	95 µg kg ⁻¹	Nriagu (1989)	0.26 [0.13-1.3] (3.3)	0.02-1.7 ^a
Volcanoes	12E-4 Mn/S	Nriagu (1989)	3.9 [2.0-20] (47)	4.2-80 ^b
Primary biogenic particles	60 mg kg ⁻¹	Nriagu (1989)	2.0 [1.0-10] (2.3)	4-50 ^a
Wildfires	Fine: 0.23 mg g ⁻¹ Coarse: 10.58 mg g ⁻¹	This study	43 [21-210] (94)	1.2-45 ^a
Industrial dust	0.01-0.05 Mn/Fe	Rathod et al. (2019)	73 [36-360] (54)	10 ^a

261
262 *Note.* Desert and agricultural dust Mn budget values were obtained from the dust model
263 simulations which used as input the Mn composition of soils constructed using linear
264 interpolation from Section 2.1.1. Alternatively, soil-type extrapolation yielded 570 Gg yr⁻¹ and
265 230 Gg yr⁻¹ for desert dust and agricultural dust, respectively. ^aNriagu (1989). ^bMahowald et al.
266 (2018).

267 268 2.2.1 Desert Dust

269 The desert dust sources of Mn refer to mineral particles entrained into the atmosphere by strong
270 winds at the soil surface in arid unvegetated or loosely vegetated regions, where soils are prone
271 to wind erosion, and play a major role in the global aerosol budget (Vandenbussche et al., 2020;
272 Boucher et al., 2013; Zender et al., 2003). The emissions, transport, and deposition of dust
273 aerosols, including seasonal and interannual variability, are all prognostic in the model. We
274 applied the same dust emission scheme (Kok et al., 2014a, 2014b) as in Wong et al. (2021), and
275 tuned the model to obtain a global mean aerosol optical depth (AOD) of 0.03 (Li et al., 2022)
276 based on observational estimates (Ridley et al., 2016). Transport and deposition of Mn were
277 simulated separately according to the size mode (Liu et al., 2016), following treatment on dust
278 aerosols as described in Albani et al. (2014). In addition, to improve the simulation of aerosols in
279 the coarse and accumulation modes, we modified the model by using the geometric median
280 diameter (GMD) as that initialized in CAM5 and geometric standard deviation as well as the
281 edges of the predicted coarse-mode GMD following Li et al. (2022).

282

283 Because desert dust is generated from soil, we assumed that the soil Mn concentration is the
284 same as the Mn in the dust, regardless of particle size, as we had no information on the size
285 segregation of the soil Mn. With linear interpolation, we derived the amount of Mn emissions to
286 be 950 Gg yr^{-1} , which was higher than 570 Gg yr^{-1} resulting from the soil map extrapolated
287 (Table 1). Both exceeded the range ($42\text{-}400 \text{ Gg yr}^{-1}$) provided in Nriagu (1989) and the former is
288 comparable to the value (900 Gg yr^{-1}) given by Mahowald et al. (2018). This result indicated the
289 high uncertainty in the amount of Mn from dust rising from different interpolation methods and
290 the large variability in soil observations; therefore, a large range of $290\text{-}4800 \text{ Gg Mn yr}^{-1}$ was
291 assigned.

292

293 2.2.2 Agricultural Dust

294 Agricultural land use and land cover change induced by human activities can boost mineral dust
295 emissions through various mechanisms that increase soil erodibility, such as increasingly
296 exposing soil surface and altering hydrologic cycles (Ginoux et al., 2012; Webb & Pierre, 2018).
297 Satellite-based analysis suggests that it represents 25% of global dust emissions (Ginoux et al.,
298 2012). To account for agricultural dust, we applied datasets of crop fraction of present
299 agricultural land from the Coupled Model Intercomparison Project Phase 5 (CMIP5) datasets
300 (Hurtt et al., 2011). We separately computed the crop sources of dust (identified using the above
301 dataset) and tuned these sources for each region to match those estimated from satellites, with the
302 exception of Australia, where we assumed only 15% of the dust is anthropogenic, consistent with
303 other studies (e.g., Bullard et al., 2008; Mahowald et al., 2009; Webb & Pierre, 2018). The
304 discrepancy in Australia between the results of Ginoux et al. (2012) and other studies (Table S2)
305 may be caused by the large drought during the time period studied by Ginoux et al. (2012). No
306 clear evidence indicated that agriculture significantly alters the Mn concentration at the soil
307 surface. Therefore, we assumed the same Mn fraction as desert dust and used the same
308 approaches for estimation, deriving a global emissions of $390 \text{ Gg Mn yr}^{-1}$ with a range of 120-
309 $1900 \text{ Gg Mn yr}^{-1}$ (Table 1).

310

311 2.2.3 Sea spray

312 Sea spray aerosols are produced by the bubble-bursting process typically resulting from whitecap
313 generation under high wind conditions in the boundary layer (O'Dowd & de Leeuw, 2007). We
314 used prognostic sea spray included in CAM6 (Liu et al, 2011) and assumed a constant
315 concentration of $95 \mu\text{g Mn kg}^{-1}$ in sea-spray aerosols (Nriagu, 1989). Sea-spray aerosols were
316 estimated to emit $0.26 \text{ Gg Mn yr}^{-1}$ with an uncertainty range of $0.13\text{-}1.3 \text{ Gg Mn yr}^{-1}$ (Table 1),
317 falling within the range given by Nriagu (1989).

318

319 2.2.4 Volcanoes

320 Studies have shown that volcanoes can be an important contributor to trace elements in aerosols,
321 such as Mn, through eruptive activities and degassing (Mahowald et al., 2018; Sansone et al.,
322 2002). We assumed only non-eruptive sources for this study (Spiro et al., 1992), with a constant

323 source across the time periods. For volcanic sources, the concentration of trace elements is
324 commonly expressed using their ratio to sulfur (S). We adopted a mass-based ratio of 12×10^{-4}
325 Mn/S from Nriagu (1989) and multiplied it with the concentration of sulfur given in the data set
326 (Spiro et al., 1992) to derive Mn. We estimated non-eruptive volcanic emissions to be 3.9 Gg Mn
327 yr^{-1} with a range of 2.0-20 Gg Mn yr^{-1} , lying at the lower end of the range provided by Nriagu
328 (1989) (Table 1).

329

330 2.2.5 Primary Biogenic Particles

331 Primary biogenic particles (PBPs) are a diverse group of airborne particles such as bacteria,
332 fungal spores, pollen, viruses and algae that are directly released from the biosphere into the
333 atmosphere (China et al., 2020; Després et al., 2012). Like volcanoes, they are not explicitly
334 simulated in the default CAM6 model but act as a non-negligible aerosol metal source
335 (Mahowald et al., 2018). Following Brahney et al. (2015), we adopted parameterized PBP data
336 that are temporally constant and based on the assumption of a leaf area index dependent source
337 for vegetative and insect debris. We also included a pollen source based on (Heald & Spracklen,
338 2009) and a bacteria parameterization (Burrows et al., 2009). The emission, transport, and
339 deposition of PBPs were simulated using a separate tracer. We assumed the Mn fraction to be 60
340 mg kg^{-1} in PBPs (Nriagu, 1989) and estimated its emission to be 2.0 Gg Mn yr^{-1} with a range of
341 1.0-10 Gg Mn yr^{-1} (Table 1).

342

343 2.2.6 Wildfires

344 Aerosols emitted from wildfires can significantly contribute to atmospheric Mn (Nriagu, 1989),
345 especially in densely forested regions that are fire-prone (Krawchuk et al., 2009). Various
346 emission datasets that use satellite-based remote sensing or other black carbon (BC) proxies are
347 available for wildfires (van der Werf et al., 2004; Van Marle et al., 2017). Here, we employed
348 the Coupled Model Intercomparison Project (CMIP6) wildfire dataset as the source of BC
349 emissions (Van Marle et al., 2017), taking advantage of its coverage of both natural fires and
350 human influence on wildfires, including deforestation fires and control of current wildfires. To
351 convert BC to Mn concentrations, we calculated the Mn to BC ratios in coarse (PM10) and fine
352 (PM2.5) fractions (similar to Mahowald et al., 2005; Hamilton et al., 2022) using observational
353 data at specific sites located in the Amazon rainforest and upper southern Africa dominated by
354 wildfires (Maenhaut et al. 1999, 2000, 2002). We derived a ratio of 10.58 mg g^{-1} for the coarse
355 fraction and 0.23 mg g^{-1} for the fine fraction and estimated global wildfire contributions to be 43
356 Gg Mn yr^{-1} with a range of 21-210 Gg Mn yr^{-1} (Table 1). These values are higher than those
357 reported in Nriagu (1989) based on more observations.

358

359 2.2.7 Industrial Emissions

360 Industrial emissions of Mn include anthropogenic fossil-fuel combustion, biomass burning, and
361 related activities. Because Mn has many biogeochemical properties similar to those of Fe
362 (Canfield et al., 2005), we assumed the co-occurrence of Mn with Fe and used an updated

363 detailed Fe emission inventory for 2010 developed using a Speciated Pollutant Emissions Wizard
364 (SPEW) (Bond et al., 2004; Rathod et al., 2020). This inventory covers Fe emission from fossil
365 fuel burning, wood combustion, and smelting in the industrial, transport, and residential sectors
366 globally (Alves et al., 2011; Arditoglou et al., 2004; Block & Dams, 1976; Córdoba et al., 2012;
367 Davison et al., 1974; de Souza et al., 2010; Dreher et al., 1997; Hansen et al., 2001; Huffman et
368 al., 2000; Koukouzas et al., 2007; Linak et al., 2000a, 2000b; Machado et al., 2006; Mamane et
369 al., 1986; Martinez-Tarazona et al., 1990; Meij, 1994; Querol et al., 1995; Schmidl et al., 2008;
370 Smith et al., 1979; Steenari et al., 1999; Stegemann et al., 2000; Tsai & Tsai, 1998; Watson et al.,
371 2001; Zhang et al., 2012). We then used estimates of the ratio of Mn to Fe in each type of source
372 to obtain a new emission inventory for Mn (Table S3). Detailed data and citations are provided
373 in Data Set S3. We estimated the global industrial emission to be 73 Gg Mn yr⁻¹ with a range of
374 36-360 Gg Mn yr⁻¹ (Table 1). There is still a large uncertainty in these first estimates of Mn, and
375 we consider elevated sources as well in later sections to better match the observational data.

376

377 2.3 Atmospheric Observations

378 Atmospheric observations of Mn concentrations in particulate matter (PM) were compiled and
379 compared with the model output to assess the performance and tune the model. We compiled
380 atmospheric Mn observational data from a variety of global dataset networks and sites
381 (Wiedinmyer et al., 2018). The available data were collected using a variety of time periods and
382 using different chemical speciation analyses as described in detail in each study (Data Set S2).
383 Most of the data were collected with size segregation between PM_{2.5} and PM₁₀ size categories
384 (e.g. Hand et al., 2019). Some observational studies used coarse (PM_{10-2.5} with aerodynamic
385 diameter between 2.5 and 10 μm) and fine (PM_{2.5}) size categories instead (e.g. Maenhaut et al.
386 1999, 2000, 2002). In this case, the two sizes were summed to compute PM₁₀ for model
387 comparison. X-ray fluorescence is the most frequently used detection method to measure Mn
388 concentrations. The Mn quantification was unavailable at some stations if concentrations were
389 lower than their method detection limit (MDL). In other sites Mn was measured using
390 Inductively coupled plasma mass spectrometry (ICP-MS). In total, we obtained more data points
391 for PM_{2.5} (N = 699) than PM₁₀ (N = 204) because many sites focused only on PM_{2.5}, such as
392 from the Interagency Monitoring of Protected Visual Environments (IMPROVE) remote/rural
393 network in the US (Hand et al., 2017; Hand, 2019). Detailed descriptions of site and method, as
394 well as other elemental/total Mn PM data can be found within each referenced study (Data Set
395 S2). While there exists limited deposition elemental data, there was not enough data to warrant
396 detailed comparisons here, and the absolute values of dry deposition were often difficult to
397 measure (Prospero et al., 1996; Schutgens et al., 2016). We ignored particles larger than 10 μm
398 in aerodynamic diameter here, because of the limited data, although the missed fraction of
399 aerosols could be important for biogeochemistry in some regions (Adebisi et al., 2023).

400

401 Hand et al. (2019) reported that collocated sites from the US Environmental Protection Agency
402 (EPA) and IMPROVE recorded different coarse aerosol mass (PM_{10-2.5}), with the value at EPA

403 sites being 10% higher than at IMPROVE sites and a 28% difference between these estimates,
404 suggesting that different samplers could have different acuteness of size fractionation for PM₁₀
405 and PM_{2.5} (Hand et al., 2019). Overall, with a correlation coefficient of 0.9 and a slope of 0.9, the
406 two sets of sites agreed with each other, but the difference brought by sampler biases should still
407 be noted during later analysis and evaluation (Hand et al., 2019).

408

409 For comparison with the model, we computed annual means of atmospheric Mn concentration
410 for each site. Particulate Mn has very low concentrations ($< 1 \mu\text{g}\cdot\text{m}^{-3}$), and therefore in many
411 cases the data can be below the detection limit. We applied the same procedure used by Wong et
412 al. (2021) to correct for this potential bias. If a site had more than half of its data values above
413 the detection limit, we set the value of any samples below MDL at this site to be one-third of the
414 MDL (shown in dataset S2). If more than 50% of the data was below the MDL at a site, we did
415 not include it in comparison to the model. These data were instead used to compute an upper
416 bound based on their respective detection limits. Since many sites were close together in regions
417 such as Europe and US, to better display the data and show the model comparison, observational
418 data from different sites were averaged spatially within a grid cell that was two times the model
419 resolution, or $\sim 2^\circ \times 2^\circ$ (Schutgens et al., 2016).

420

421 2.4 Estimation of “Pseudo” Turnover Time

422 The importance of atmospheric Mn deposition to the soil Mn reservoir was evaluated by
423 calculating the soil Mn turnover time, which is defined as the total mass of soil Mn (estimated to
424 1 m depth) in each grid cell divided by the estimated atmospheric deposition flux from
425 simulation. The Mn mass was calculated using the Mn concentration from both estimated soil
426 maps multiplied by an average bulk density of soil, 1.4 g cm^{-3} (Yu et al., 1993). The turnover
427 time estimated here is “pseudo-turnover time” (Wong et al., 2021) because we could not assume
428 soil Mn to be in a steady state. The characterization of the turnover time and comparison on a
429 global scale allowed us to assess the ecological significance of atmospheric Mn deposition in the
430 soil Mn reservoir in units of years (Okin et al., 2004).

431

432 2.5 Correlation Analysis and Interpretation of Ecological Relevance

433 Whalen et al. (2018) suggested Mn limitation as a mechanism for reduced decomposition under
434 enhanced atmospheric N deposition, therefore, it might be helpful to consider Mn deposition
435 together with N deposition. We adopted a modeled annual N deposition dataset ($2^\circ \times 2^\circ$)
436 (Brahney et al., 2015b) and re-gridded our model output of the Mn deposition onto its resolution
437 ($2^\circ \times 2^\circ$), followed by raster calculation of the ratio of atmospheric Mn deposition to N
438 deposition, which might provide useful insights for the relative susceptibility of soil to Mn
439 limitation following N deposition. We compared the Mn over N ratio in deposition to the
440 concentration ratio in soils using total N concentration data at available NCSS sites. The ratio
441 was computed using both natural Mn deposition and total Mn deposition (natural +
442 anthropogenic) to understand how and where human activities altered this ratio.

443
444 To examine how atmospheric Mn deposition potentially influences the Mn limitation that could
445 be related to decomposition and soil C storage in forest ecosystems (Kranabetter et al., 2021;
446 Moore et al., 2021; Stendahl et al., 2017; van Diepen et al., 2015; Whalen et al., 2018), we
447 performed a spatial correlation analysis between Mn deposition and topsoil (0-5 cm) C density
448 derived from SoilGrids 2.0, a digital soil database that includes 230,000 soil profile observations
449 from the WoSIS and applies machine learning methods (Poggio et al., 2021) to map the global
450 distribution of soil properties at 250 meters, resampled to our model resolution ($1^\circ \times 1^\circ$). We
451 identified the ecosystem type at each grid cell using the plant functional types in the Community
452 Land Model, version 5 (Lawrence et al., 2019), taking the rubric of having more than 80 percent
453 of the area covered by forest biomes. Because different forest ecosystems may have distinct soil
454 Mn status and limitation conditions (Berg et al., 2010), they were divided into three subsystems:
455 temperate forests, tropical forests, and boreal forests, with the correlation analysis conducted
456 both combinedly and separately.

457
458 Because soil organic matter decomposition has long been understood to be controlled by a
459 combination of several different factors, Mn deposition cannot be interpreted separately from
460 other commonly outlined predictors such as precipitation (moisture), temperature, and N
461 deposition (Berg & Matzner, 1997a; Frey et al., 2014; Hartley et al., 2021; Sierra et al., 2015;
462 Woo & Seo, 2022; Zak et al., 2017; Zhang et al., 2019; Zhao et al., 2021b). To include these
463 potential constraints, simple and multilinear regression analyses were carried out with the
464 addition of the 3 other factors: precipitation, temperature (long-term mean data from Terrestrial
465 Air Temperature and Precipitation: 1900-2014 Gridded Monthly Time Series data provided by
466 the NOAA PSL, Boulder, Colorado, USA, from their website at <https://psl.noaa.gov>), and N
467 deposition to test the significance of Mn deposition on topsoil C storage. The multilinear
468 regression was calculated following the ordinary least squares (OLS) method.

469 **3 Results**

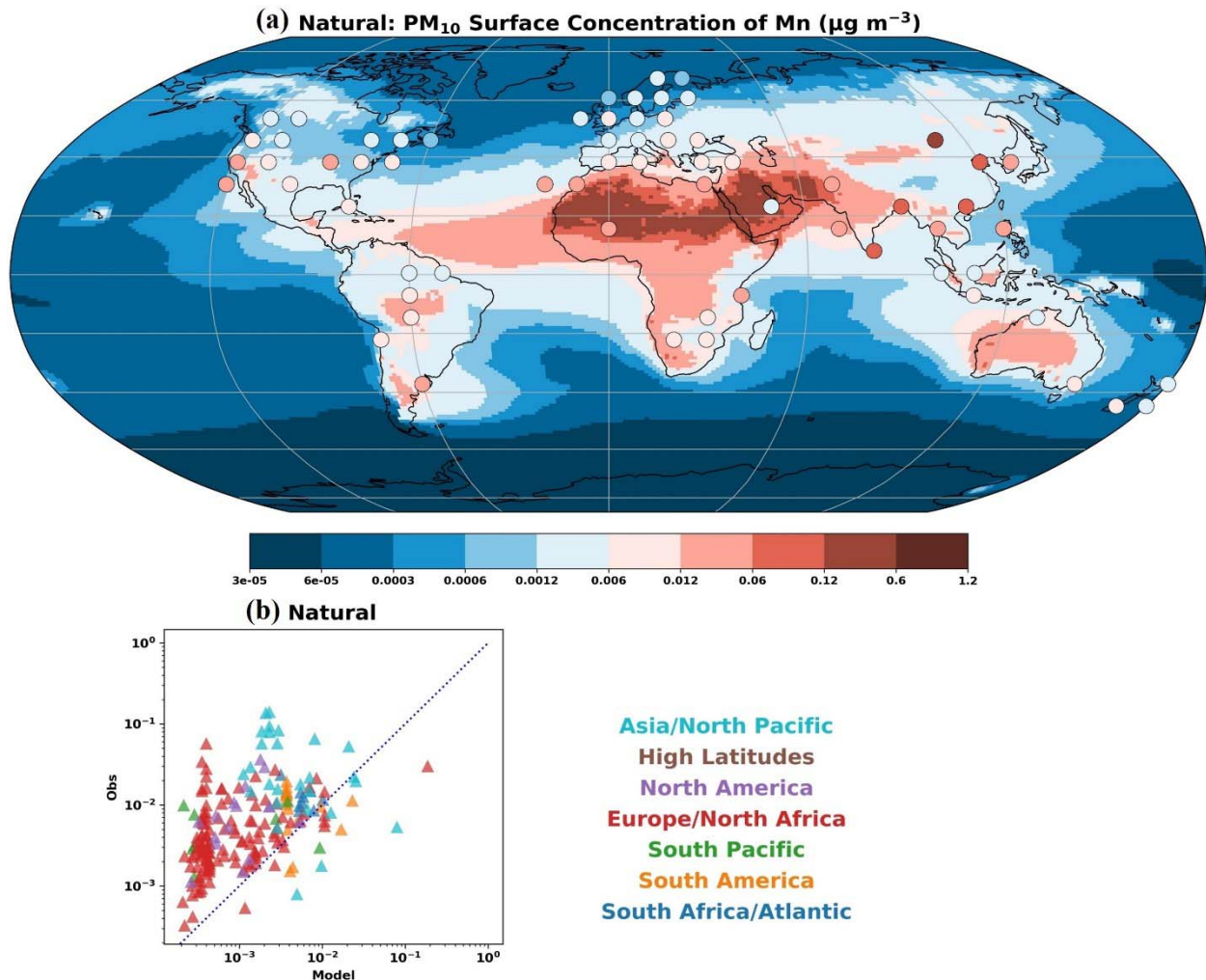
470 **3.1 Mn Concentration in Atmospheric Particulate Matter (PM)**

471 Mn in the model output was compared with the Mn concentration in atmospheric PM
472 observation on a global scale. Here, we present three cases (Figures 2 and 3) for the simulation
473 with dust emission schemes created by linear interpolation (Section 2.1.1) to better examine the
474 model sensitivity to anthropogenic emissions. We used the bounded observational data (Section
475 2.3) for all comparisons and scatter plots.

476
477 The natural case (Figure 2a) was simulated without any emission from anthropogenic sources
478 (industrial emission + agricultural dust). With only natural contributions, the model
479 underestimated Mn concentration significantly in the PM₁₀ size fraction (Figure 2b), especially
480 over industrialized regions in Asia, Europe, and southern Africa, where the world's largest Mn
481 mining industry is located (U.S. Geological Survey, 2022). The model also poorly simulated the

482 relatively high Mn concentrations reported by several sites across North America. Only close to
483 dust desert dominated regions in North Africa does the model simulate the concentrations well
484 (Figure 2a). The spatial distribution of Mn in western North Africa agrees with the observations
485 on the location Mn rich dust sources (Rodríguez et al., 2020).

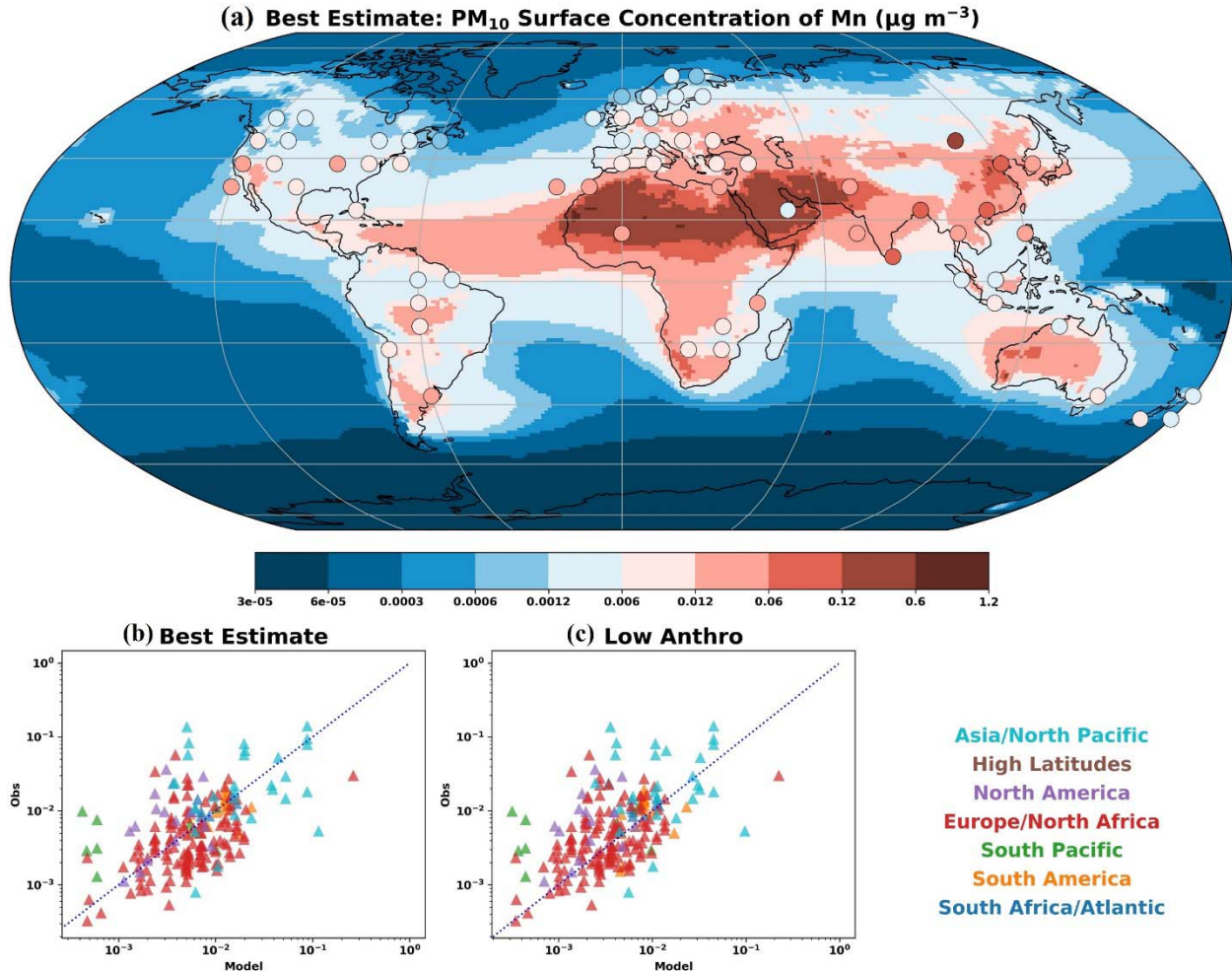
486
487 When anthropogenic sources were added, using the default values described in Section 2.2, the
488 model improved the simulation in industrialized regions (Figure 3b). The value of the correlation
489 coefficient (r) increased 3-fold with root mean squared error on the same level (RMSE) ($r =$
490 0.089 , $RMSE = 0.025$ in Figure 2b; $r = 0.27$, $RMSE = 0.023$ in Figure 3b), suggesting that the
491 model performance improved with the addition of anthropogenic contributions. However, Mn
492 concentrations at the major proportion of sites were still underestimated compared with the
493 observations. Using trial and error, we found that the atmospheric concentrations were best
494 matched when we increased the anthropogenic emissions by a factor of 2. In comparison,
495 adjusting natural sources only had a minimal effect on improving the overall model performance
496 and could sometimes lower the accuracy. Natural sources other than desert dust and wildfires
497 contributed little to the total aerosol budget (Table 1), and the most underestimated industrial
498 regions were barely subjected to aerosol deposition associated with desert dust or wildfires. We
499 define our “best case” as the case with elevated anthropogenic emissions (Figures 3a and b) and
500 denoted the unmodified scenario the “low anthro” case (Figure 3c). While some stations were
501 overestimated in the best estimate case, much fewer stations were, and the data spots were
502 distributed more uniformly along the 1:1 line of the scatter plots, with r increased to 0.36. In
503 many of the sites, there was a mismatch between the date of the measurement and the model
504 simulation because of limited observations.



505
 506 **Figure 2.** (a) Global distribution of the atmospheric Mn concentration at the surface in the PM₁₀
 507 size fraction from the model simulation results (contours) using only natural sources with a dust
 508 scheme constructed by linear interpolation and from bounded observations (circles).

509 Observations were spatially averaged to a $\sim 2^\circ \times 2^\circ$ grid and compared to the Community
 510 Atmosphere Model (CAM) (v6) results. (b) Scatterplot comparison of model simulated
 511 atmospheric concentration with observations in the natural case ($n = 203$, $r = 0.089$, $\text{RMSE} =$
 512 0.025). Colors of points indicate the locations of studies listed in the legend.

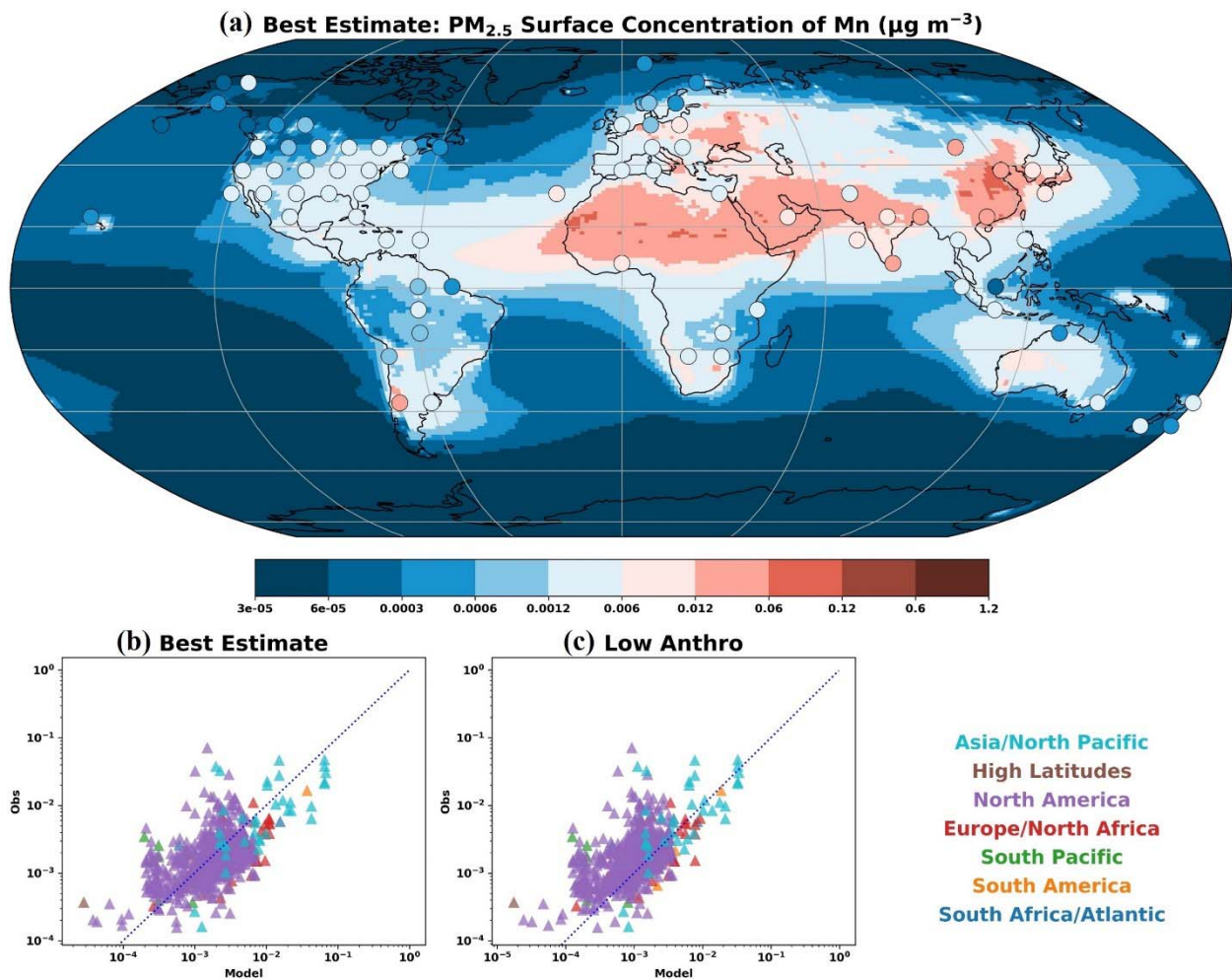
513
 514 We noticed that a few sites with high Mn concentrations across North America including several
 515 peaks in the central United States, were still missed by the model in the best estimate case,
 516 suggesting that our estimation of anthropogenic source contributions could be lower than the
 517 actual in this region. Overall, our model agreed on the same order of magnitude of Mn
 518 concentration in atmospheric PM₁₀ as the observations and had the ability to, at least, partially
 519 represent the variability in their spatial distribution.



520
 521 **Figure 3.** (a) Global distribution of the atmospheric Mn concentration at the surface in the PM₁₀
 522 size fraction from the model simulation results (contours) using the dust scheme constructed by
 523 linear interpolation in the best estimate case and from bounded observations (circles).
 524 Observations were spatially averaged to a $\sim 2^\circ \times 2^\circ$ grid and compared to the Community
 525 Atmosphere Model (CAM) (v6) results. (b) Scatterplot comparison of model simulated
 526 atmospheric concentration with observations in the best estimate case ($n = 203$, $r = 0.36$, $\text{RMSE} = 0.025$).
 527 Colors of points indicate the locations of studies listed in the legend. (c) Same as (b),
 528 except for the low anthropogenic model case ($n = 203$, $r = 0.27$, $\text{RMSE} = 0.023$).

529
 530 Despite the dominance of the PM₁₀ size fraction of the atmospheric Mn budget due to the coarse
 531 nature of dust (Table 1), Mn in atmospheric PM_{2.5} is also important because of the high
 532 percentage of fine fraction in wildfires and industrial dust (Table 1) and the potential health risks
 533 that could be induced by inhalation of Mn in PM_{2.5} in ambient air (Cavallari et al., 2008;
 534 Expósito et al., 2021). Generally, we obtained similar global distribution patterns and results of
 535 the model-observation comparison as in PM₁₀. With a more than tripled number of atmospheric
 536 Mn observations in the PM_{2.5} size fraction, especially in the U.S., the model simulation better
 537 matched the observations across North America (Figure 4a). The highest observation values

538 were reported over industrialized regions in Europe and Asia and regions affected by desert dust
 539 generated in North Africa. Our model showed elevated atmospheric Mn levels in Europe and
 540 Asia compared to the Americas. Similarly, atmospheric Mn over industrialized regions was
 541 underrepresented by the model simulations in the natural case (Figure S2), and we derived our
 542 best estimate by tuning the level of anthropogenic emissions towards the higher end by a factor
 543 of 2. With the best estimate case, our model showed a moderately good representation of the
 544 observations (Figure 4b and c). Having more observational sites might explain the slightly better
 545 performance of the comparison in the PM_{2.5} size fraction than in the PM₁₀ size fraction.
 546



547
 548 **Figure 4.** Same as Figure 3, but for the PM_{2.5} size fraction. (a) Global distribution of the
 549 atmospheric Mn concentration at the surface from the model simulation results (contours) using
 550 the dust scheme constructed by linear interpolation in the best estimate case and from bounded
 551 observations (circles). Observations were spatially averaged to a $\sim 2^\circ \times 2^\circ$ grid and compared to
 552 the Community Atmosphere Model (CAM) (v6) results. (b) Scatterplot comparison of model
 553 simulated atmospheric concentration with observations in the best estimate case ($n = 698$, $r =$
 554 0.53 , $\text{RMSE} = 0.006$). Colors of points indicate the locations of studies listed in the legend. (c)
 555 Same as (b), except for the low anthropogenic model case ($n = 698$, $r = 0.53$, $\text{RMSE} = 0.005$).

556

557 We performed the same analysis using model simulations with a percent Mn in dust using soil-
558 type extrapolation (Section 2.1.2) and found the results changed quantitatively but not qualitatively
559 (Figure S3). Both methods produced simulation results that were on the same order of magnitude
560 as the observations.

561

562 3.2 Atmospheric Mn Budget and Source Apportionment

563 Our model predicted the global total Mn emission to be 1500 Gg Mn yr⁻¹ with a range of 460-
564 7300 Gg Mn yr⁻¹ due to the uncertainty in each source (Table 1). The estimate was similar in
565 magnitude to the reference value of 1000 Gg Mn yr⁻¹ given by Mahowald et al. (2018). The
566 model-simulated budget for each source was within or close to the estimated range from previous
567 studies (Mahowald et al., 2018; Nriagu, 1989). The model estimated that 1000 Gg Mn yr⁻¹ was
568 emitted from natural sources with a range of 310-5000 Gg Mn yr⁻¹, while 460 Gg Mn yr⁻¹ was
569 emitted from anthropogenic sources with a range of 150-2300 Gg Mn yr⁻¹ (Table 1), suggesting
570 that approximately 32% (best estimate case) of the atmospheric Mn arose from anthropogenic
571 contribution.

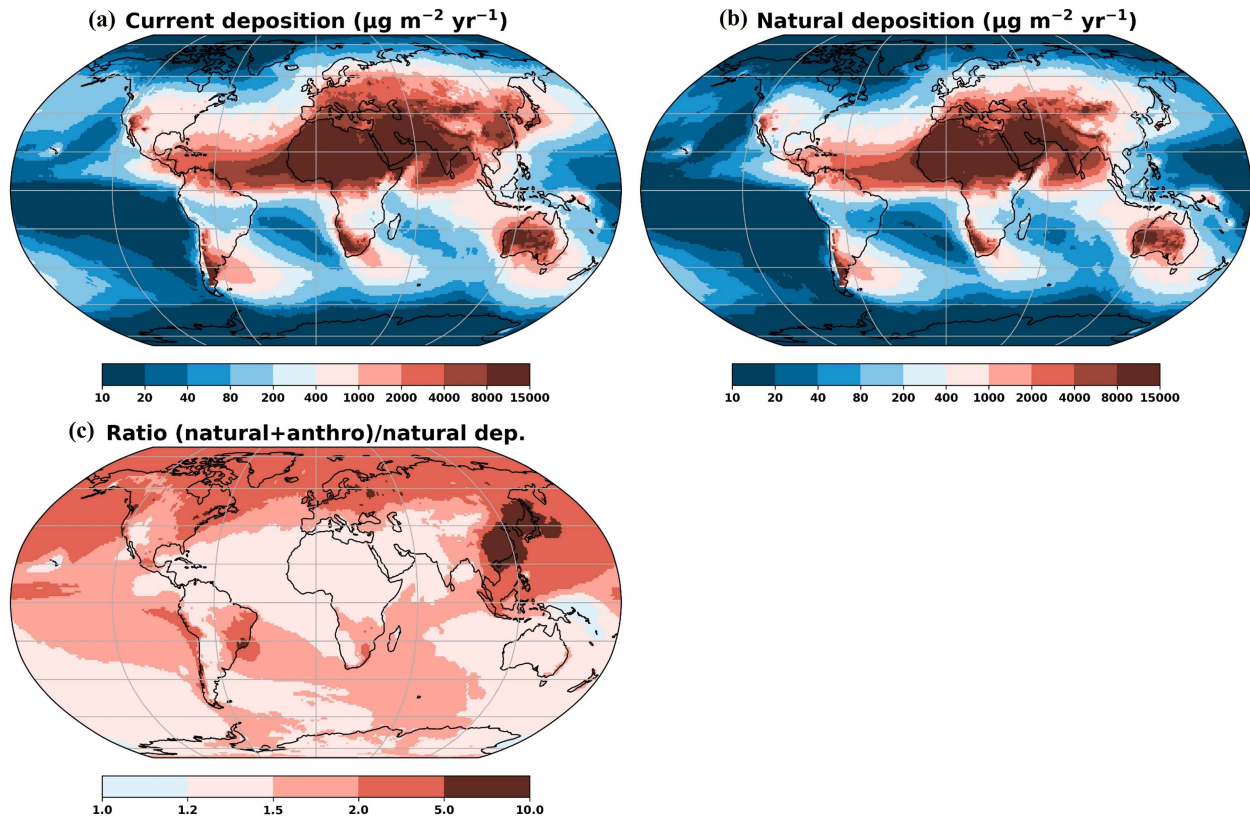
572

573 While anthropogenic sources contributed to a significant portion of the total atmospheric Mn
574 budget, our model suggested that their main influence was in the Northern Hemisphere, where
575 the ratio of total to natural deposition was significantly greater than 1 (Figure 5), and there was a
576 high percentage of anthropogenic or industrial dust (Figures 6c and d), especially over
577 industrialized regions in Asia, Europe, and the northeastern U.S. Hot spots in the Southern
578 Hemisphere included eastern and southeastern Brazil, Peru, Chile, and southern Africa. High
579 ratios of total to natural deposition in these regions indicated strong human perturbations (up to
580 10 times higher) on the Mn deposition rates (Figure 5c). Industrial emissions were responsible
581 for major regions dominated by anthropogenic deposition, while the distribution of agricultural
582 deposition was more dispersed, with a wider coverage of cultivated areas worldwide (Figures 6c
583 and d).

584

585 Desert dust represented over 90% of all natural sources of the atmospheric Mn deposition (Table
586 1). It dominated deposition within major deserts in North Africa, inland Australia, and Asia as
587 well as regions that were affected by the transportation of desert dust produced in these systems
588 (Kellogg & Griffin, 2006). For example, the intercontinental transport of African dust to South
589 America has been identified as an important source of new atmospheric deposition of P in the
590 Amazon and could have a fertilization effect (Okin et al., 2004; Ridley et al., 2012; Yu et al.,
591 2015). The dominance of desert dust and other natural sources (sea salts and volcanoes, which
592 represented a very small fraction) was complementary with anthropogenic sources: desert dust
593 dominated most of the Southern Hemisphere but became less influential at higher latitudes in the
594 Northern Hemisphere as anthropogenic emissions concentrated there (Figure 6a).

595



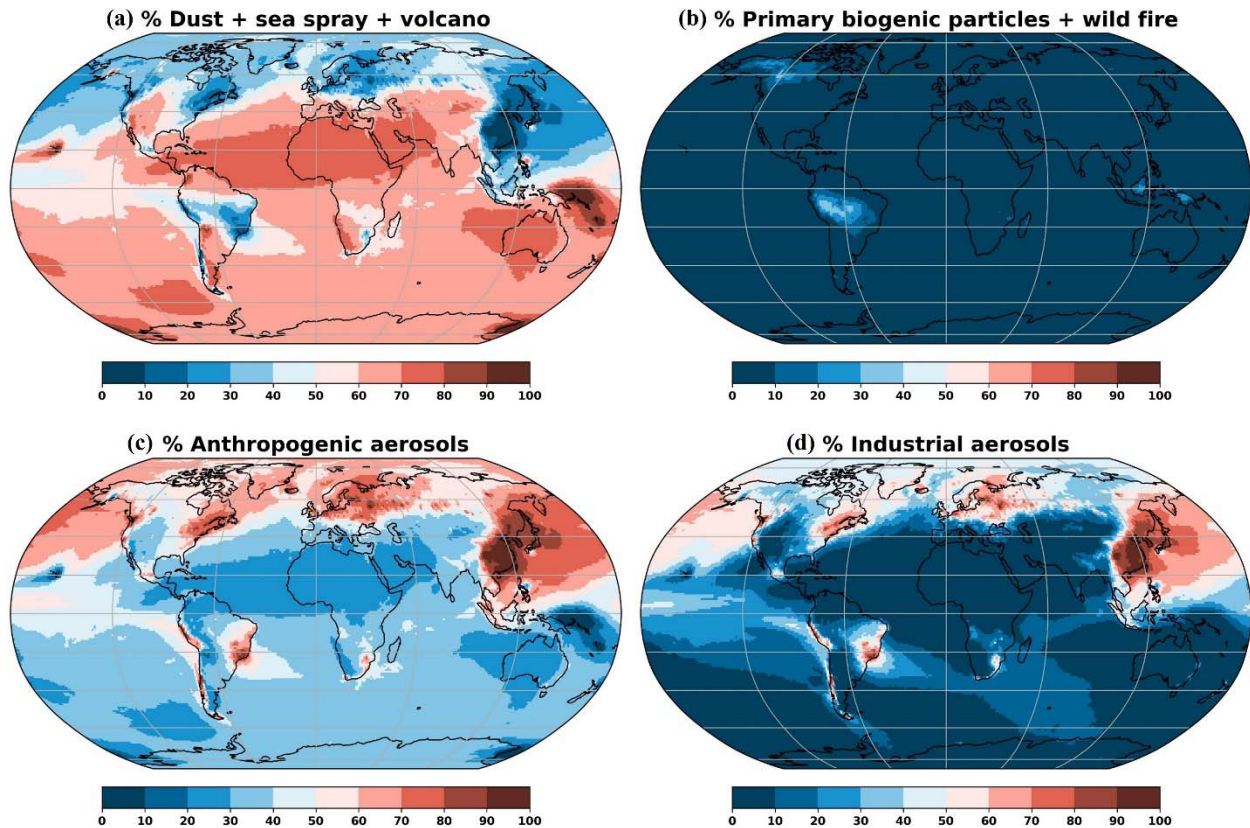
596

597 **Figure 5.** (a) Global pattern of the current (anthropogenic + natural sources) atmospheric Mn
 598 deposition ($\mu\text{g m}^{-2} \text{yr}^{-1}$) as simulated in the Community Atmosphere Model (CAM) (v6) in the
 599 best estimate case. (b) Same as (a), except for including natural sources of emissions only. (c)
 600 Ratio of total atmospheric Mn deposition to natural deposition.

601

602 Although wildfires have a much lower budget than desert dust, they are the second-largest
 603 natural source of atmospheric Mn (Table 1). Together with primary biogenic particles, they
 604 dominated regions such as the Amazon rainforest, upper southern Africa (and Madagascar),
 605 Indonesia, northern Canada and Alaska (Figure 6b). Wildfires can displace large amounts of
 606 nutrients, including Mn, from terrestrial ecosystems (Kauffman et al., 1995; Mahowald et al.,
 607 2005) which were then replenished by transported dust and sea salts, as well as anthropogenic
 608 depositions, similar to what was reported by Wong et al. (2021) in the case of molybdenum (Mo).

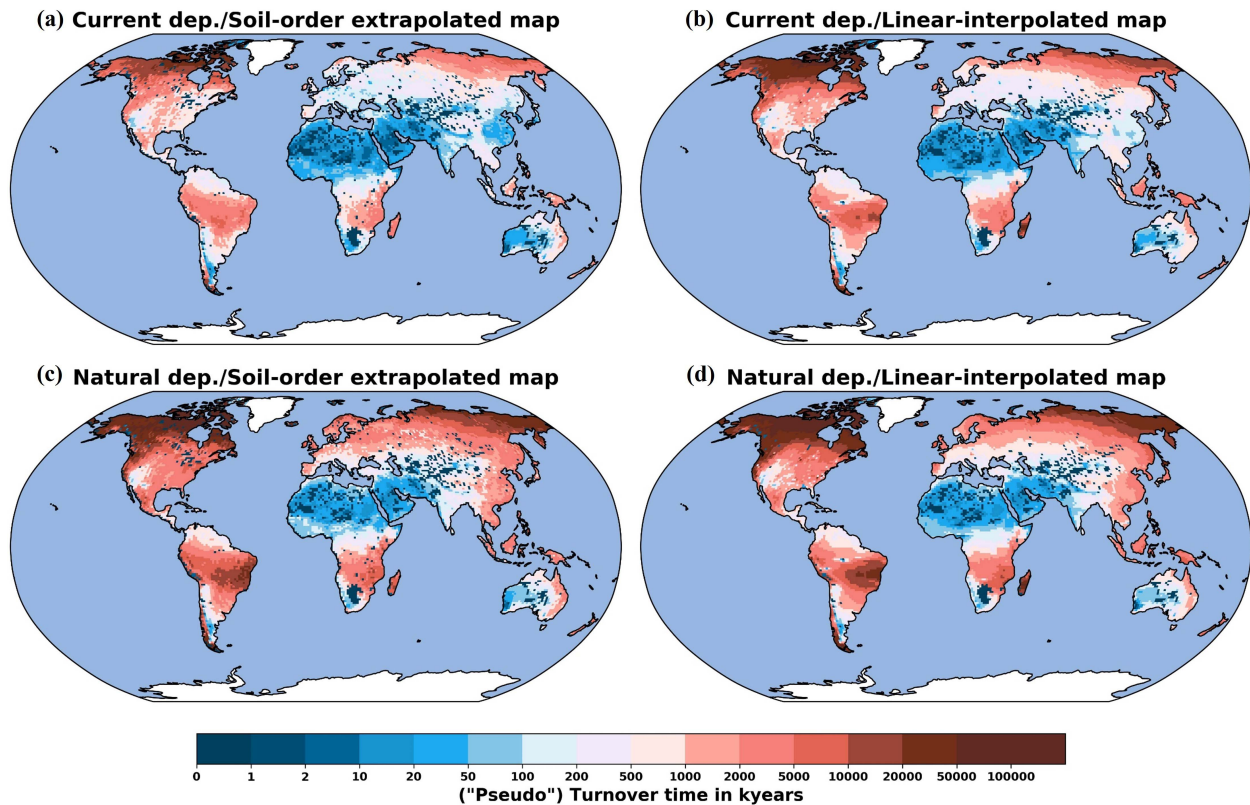
609



610
 611 **Figure 6.** Source apportionment of the atmospheric Mn deposition in the best estimate case
 612 shown by percentage of different sources in the Community Atmosphere Model (CAM) (v6): (a)
 613 desert dust, sea sprays, and volcanoes, (b) primary biogenic particles and wildfires, (c) combined
 614 anthropogenic aerosols (agricultural dust + industrial emissions) and (d) industrial aerosols.
 615

616 3.3 Soil Mn “Pseudo Turnover” Times

617 The “pseudo” turnover time provides a metric of the ecological importance of atmospheric Mn
 618 deposition to the topsoil Mn reservoir (Okin et al., 2004). Using the two approaches (Section 2.1),
 619 we divided the estimated soil Mn concentration by the model simulated Mn deposition rates to
 620 compute “pseudo” turnover times in topsoils (Okin et al., 2004). The estimated soil Mn “pseudo”
 621 turnover time varied spatially, ranging from 1,000-10,000 years in regions dominated by desert
 622 dust to over 10,000,000 years at higher latitudes (Figures 7a and b). We found that anthropogenic
 623 sources significantly shortened the soil Mn “pseudo” turnover times in industrialized regions
 624 regardless of the interpolation method. For example, the atmospheric deposition sourced from
 625 anthropogenic emissions shortened the soil Mn “pseudo” turnover time by 1-2 orders of
 626 magnitude from millions of years to as low as tens of thousands of years in eastern China and
 627 across Europe (Figures 7a and c; b and d). These trends indicate that human perturbation has the
 628 potential to accelerate Mn turnover in different terrestrial systems if the amount of anthropogenic
 629 activity remains at the same level or even rises in the future.
 630



631
 632 **Figure 7.** “Pseudo” turnover times (kiloyears) of the surface soil Mn from current (natural +
 633 anthropogenic sources) atmospheric Mn deposition as simulated in the Community Atmosphere
 634 Model (CAM) (v6) using the dust scheme constructed from (a) linear interpolation (and
 635 calculated using the linear-interpolated soil Mn map) and (b) soil order extrapolation (and
 636 calculated using the soil-order extrapolated soil Mn map). (c and d) Same as (a and b) except for
 637 the inclusion of only natural Mn deposition in the calculation of turnover times.

638
 639 Compared to the Mo “pseudo” turnover time of 1,000-2000,000 years (Wong et al., 2021), the
 640 estimated range of soil Mn “pseudo” turnover times was wider, and the mean turnover time was
 641 longer, which is closer to the estimated range of P “pseudo” turnover time ($\sim 10^4$ to $\sim 10^7$ years) in
 642 Okin et al. (2004). In the Amazon region, the soil Mn “pseudo” turnover time ranged from
 643 hundreds of kiloyears in the northeast corner, which was subject to deposition from transported
 644 African dust, to thousands of kiloyears moving toward the central and southwestern regions.
 645 Compared to the turnover times from other studies of macronutrients, the estimated Mn “pseudo”
 646 turnover time here was orders of magnitude longer than the N turnover time of 177 years
 647 globally (Rosswall, 1976) and the P turnover time of 50 years averaged across several stations in
 648 the Amazon rain forest (Mahowald et al., 2005), which was accelerated by human-induced land
 649 use change such as deforestation and biomass burning (Andela et al., 2017; Hansen et al., 2013).
 650 Overall, these comparisons illustrate the spatial variability of the soil Mn “pseudo” turnover
 651 times and suggest that atmospheric deposition of Mn may play a non-negligible role in the
 652 terrestrial surface Mn cycle in many regions world-wide.

653

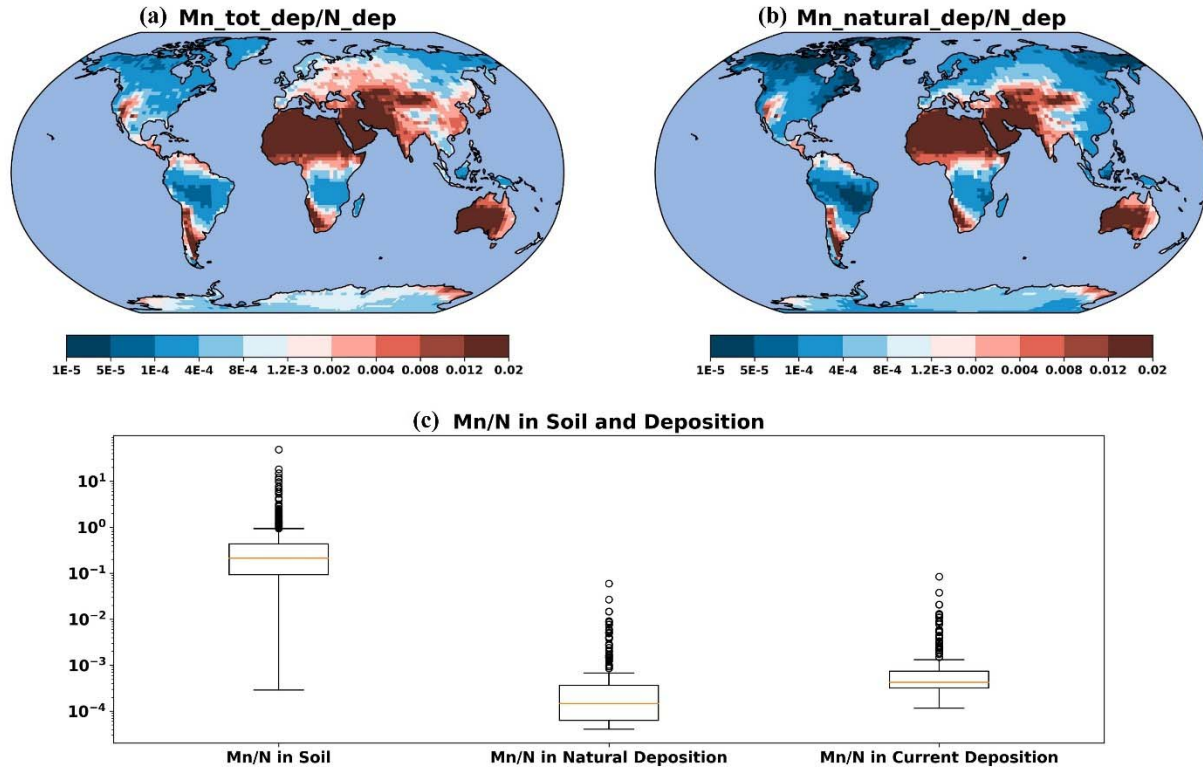
654 3.4 Linkage to N deposition and C storage

655 3.4.1 Mn to N Ratio in Deposition

656 In addition to characterizing the atmospheric Mn cycle itself, it is important to look at its linkage
657 to the biogeochemical cycles of two major elements, C and N. The Mn limitation has been
658 proposed to explain the reduced organic matter decomposition in soils under chronic atmospheric
659 N deposition (Moore et al., 2021; Whalen et al., 2018), which has the potential to regulate carbon
660 sequestration in forest soils. Therefore, using the N deposition/concentration ratio to normalize
661 the Mn deposition/concentration ratio (deriving Mn-to-N ratios) could make our results more
662 interpretive in such a way that it could reveal the soil's vulnerability to the Mn limitation (if N is
663 sufficient) and thus relates to soil C dynamics. As anthropogenic emissions have significantly
664 perturbed the cycling of atmospheric N (Dentener et al., 2006; Galloway et al., 2014; Kanakidou
665 et al., 2016) and Mn, it is likely that humans have also altered this ratio of Mn to N, affecting soil
666 C accumulations and introducing further feedbacks on climate.

667

668 The ratio of Mn to N in the atmospheric deposition varies globally by several orders of
669 magnitude. It could be as low as 5×10^{-5} in the northern latitudes and over 0.02 in desert dust
670 dominated regions, where there is little nitrogen fixation in soils, and the dust composition is
671 almost entirely of mineral nature (Davies-Barnard & Friedlingstein, 2020). Anthropogenic
672 emissions increased the depositional ratio of Mn to N in most parts of the world (even in
673 Antarctica), with the impact in industrialized regions being the most substantial (Figure 8a).
674 When only considering the natural sources, we estimated that the Mn-to-N ratio is moderately
675 low in major industrialized regions including northern Europe, eastern China, and the
676 northeastern U.S., with the U.S. having lower ratios than Asia and Europe in general (Figure 8b).
677 Anthropogenic sources enhanced the Mn-to-N ratio in all these regions, with a stronger effect in
678 China and Europe than in the U.S. Other areas with low Mn-to-N ratio under current deposition
679 were either around the equator, where much nitrogen fixation occurred (Davies-Barnard &
680 Friedlingstein, 2020), or at higher latitudes. These regions were generally affected only by desert
681 and anthropogenic dust and had relatively large wildfire and PBP contributions in deposition
682 (Figure 6b). This could be best illustrated in the Amazon forest, where the northernmost portion
683 influenced by African dust transportation (Ridley et al., 2012) had a much higher Mn-to-N ratio
684 than the central part (Figures 8a and b).



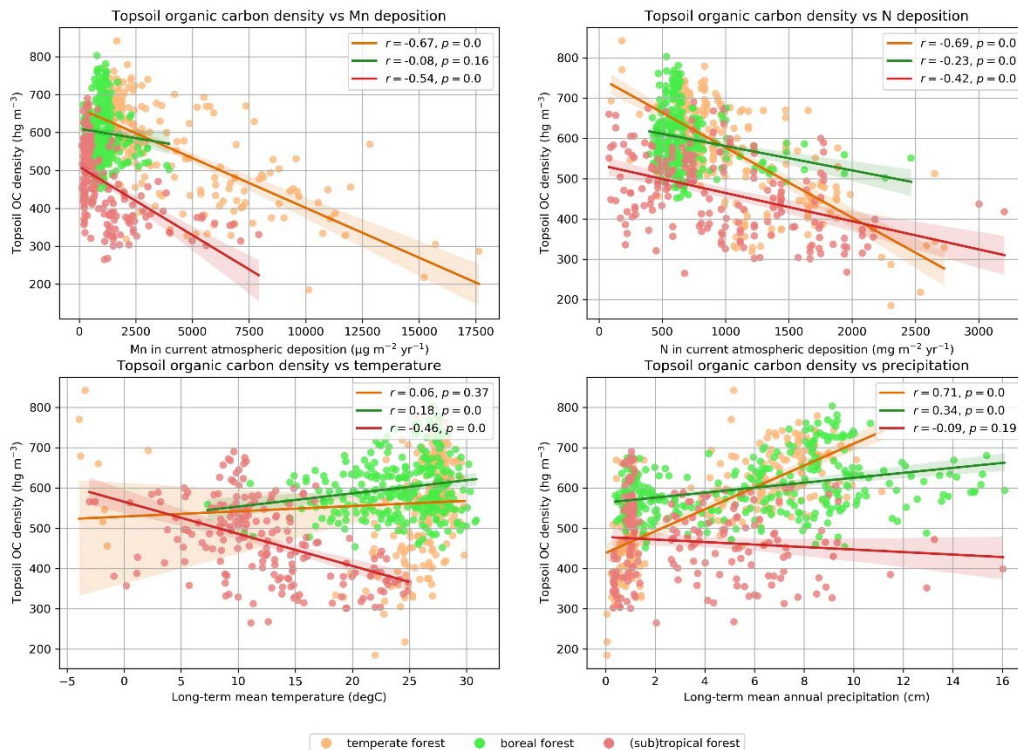
685
 686 **Figure 8.** (a) Ratio of Mn to N in atmospheric deposition calculated using the current Mn
 687 deposition simulated in the Community Atmosphere Model (CAM) (v6) and the N deposition
 688 from Brahney et al. (2015b). (b) Same as in (a), except for the inclusion of only natural Mn
 689 deposition in the calculation. (c) Box plot showing the Mn-to-N ratio in surficial soils at
 690 available sites and in depositions (current + natural).

691
 692 We compared the M-to-N ratio in atmospheric deposition to the in-situ ratio of Mn to N
 693 concentration in surficial soils at 1319 available sites (mainly across the U.S.). For example,
 694 Kranabetter et al. (2021) reported 541 mg kg^{-1} Mn and 0.77% total N in surficial soils in a
 695 temperate forest located on southern Vancouver Island. With the measurements in the
 696 abovementioned study, we calculated the in-situ Mn-to-N ratio in soil to be 0.068, which was
 697 over two orders of magnitude larger than the depositional Mn-to-N ratio of 0.00052 calculated
 698 using our gridded model output and the N deposition dataset (extracting the value of the grid in
 699 which Vancouver Island was located). Considering all available soil observational sites that
 700 contained valid measurements of Mn and N concentrations (mainly from the NCSS dataset), we
 701 obtained a median depositional Mn-to-N ratio of 0.00042 versus a median soil Mn-to-N ratio of
 702 0.21. We found that the current depositional ratio was typically one to three orders of magnitude
 703 lower than the soil concentration ratio, and the difference was larger with natural deposition
 704 (Figure 8c). Considering the relatively higher Mn-to-N ratio in soils, regions with
 705 disproportionately low Mn-to-N ratios in atmospheric deposition were interpreted to be the most
 706 vulnerable to potential Mn limitation (if deposition makes soil N sufficient), such as temperate

707 and boreal forests in northeastern U.S., Canada, and northern Europe, in agreement with current
 708 field experimental results (Kranabetter et al., 2021; Stendahl et al., 2017; Whalen et al., 2018).
 709

710 3.4.2 Correlation with Topsoil C Density

711 To test the significance of atmospheric Mn deposition in removing soil Mn limitation and thus
 712 facilitating decomposition in forest ecosystems on a global scale, we correlated our simulated
 713 atmospheric Mn deposition with the topsoil (0-5 cm) C density derived from SoilGrids 2.0
 714 (Poggio et al., 2021), with both values extracted from grid cells where the plant functional type
 715 was identified as (sub)tropical, temperate, or boreal forest. In each case, a simple linear
 716 regression between topsoil C density and each of the four factors was carried out, including Mn
 717 deposition. Our results revealed fairly good negative correlations ($r < -0.5$) between C density
 718 and Mn deposition in temperate ($r = -0.67$) and (sub)tropical forests ($r = -0.54$; Figure 9a). A
 719 similar negative relationship was determined between C density and N deposition in temperate
 720 forests ($r = -0.69$; Figure 10b), where a significant positive relationship was obtained in the case
 721 of precipitation ($r = 0.71$; Figure 10d). In addition, a negative correlation between C density and
 722 temperature was found only in subtropical forest, though relatively weaker ($r = -0.46$; Figure
 723 10c). When we combined the three forest ecosystems for simple regression analysis, all factors
 724 showed statistically significant correlation, with Mn deposition ($r = -0.37$, $p < 0.0001$) having the
 725 third strongest coefficient of determination (Table 2).



726
 727 **Figure 9.** Scatterplots with simple linear regression lines between topsoil (0-5 cm) C density (hg
 728 m⁻³) and (a) Mn in current atmospheric deposition ($\mu\text{g m}^{-2} \text{yr}^{-1}$), (b) N in current atmospheric
 729 deposition ($\text{mg m}^{-2} \text{yr}^{-1}$), (c) long-term mean temperature ($^{\circ}\text{C}$), and (d) long-term mean annual

730 precipitation (cm) in temperate, boreal, and tropical forests. “ $P = 0.0$ ” legend suggests a p-value
 731 < 0.0001 .

732

733 Results from multilinear regression confirmed the negative relationship between C density and
 734 Mn deposition to remain statistically significant along with the inclusion of the other factors into
 735 the model (Table 2). Overall, the R-squared value of the OLS model reached 0.434, with the
 736 skew (-0.115), kurtosis (3.033), and Jarque-Bera test (1.506, $p = 0.471$) likely indicating
 737 normally distributed residuals. To check for multicollinearity, we computed a correlation matrix
 738 (Table S4) and found a positive correlation between Mn deposition and N deposition ($r = 0.61$, p
 739 < 0.0001), providing the possibility that the negative correlation between C storage and Mn
 740 deposition was a “byproduct” of the positive correlation between Mn and N deposition. A
 741 calculation of variance inflation factors (VIF) obtained values < 2 for all individual variables
 742 (Table S4), suggesting that variables were only moderately correlated with each other, and
 743 multicollinearity was likely not problematic. Therefore, it is reasonable to conclude that the Mn
 744 deposition could be a predictor of topsoil C density along with N deposition and other climatic
 745 factors in forest ecosystems (predominantly temperate and tropical). In fact, Mn addition to soils
 746 has been shown to increase C losses (e.g., CO_2 and dissolved organic carbon) during litter
 747 decomposition, suggesting increased Mn supply could result in decreased soil C storage (Trum et
 748 al., 2015; Jones et al., 2020).

749

750 Table 2

751 *Result statistics of simple and multilinear regression between topsoil C content and Mn*
 752 *deposition, N deposition, temperature, and precipitation.*

<i>Variable Name</i>	Simple linear regression		multilinear regression		
	r	p-value	coef	t	P > t
<i>Intercept</i>			500.2603	39.248	0.000
<i>Mn deposition</i>	-0.372	< 0.0001	-0.0085	-4.369	0.000
<i>N deposition</i>	-0.493	< 0.0001	-0.0693	-7.977	0.000
<i>Temperature</i>	0.270	< 0.0001	4.1265	9.313	0.000
<i>Precipitation</i>	0.472	< 0.0001	8.8977	9.964	0.000

753

754

755 **4 Discussion**

756 4.1 Model-observation Discrepancy

757 Although our model simulation results had a moderately good representation of the atmospheric
 758 observations under the best estimate scenario, many stations were still under- or over-predicted
 759 (Figures 4 and 5). The discrepancy between the model and observations could arise from a
 760 variety of processes, with errors in the sources, deposition or transport pathways all contributing
 761 (Mahowald et al., 2011; Loosmore, 2003). For example, we were not able to include the
 762 emissions from direct volcanic eruptions due to the lack of data and thus constrained to apply
 763 non-eruptive degassing data only. Errors in estimates of dust deposition are thought to be of
 764 order of a factor of 10 (Mahowald et al., 2011). Because we derived Mn from industrial sources

765 from a correlation with Fe (since these are the only spatially explicit mining emissions available:
766 Rathod et al., 2019), emissions from nonferrous industries such as silico-manganese alloy,
767 synthetic pyrolusite, and Mn chemical manufacturing plants were neglected (Parekh, 1990).
768 Estimates of fugitive emissions from mining are not available, and thus not included in this study.
769

770 Another limitation was that, except for desert and agricultural dust, we used a constant emission
771 factor for each source because we did not have sufficient data to assess the spatial variability of
772 the Mn emission factors from different sources such as PBP, sea sprays, and volcanoes, which
773 could vary within the ranges given in Nriagu (1989). For example, trace element composition
774 can vary in materials formed by biological production in different water masses (Kuss &
775 Kremling, 1999). With the constant emission factor assumption, our model could over- or
776 underestimate the observations, depending on the location of the site and its source
777 apportionment.
778

779 Our regression model was not able to determine a statistically significant negative correlation
780 between topsoil C density and our simulated atmospheric Mn deposition in boreal forests. This
781 seems contradictory with the results from a direct observational study carried out in northern
782 Swedish boreal forests, where Mn was found to act as a critical factor regulating C accumulation
783 (Stendahl et al., 2017). This apparent discrepancy might be attributed to the limited number of
784 soil observations within the boreal regime, introducing large uncertainty at the higher latitudes in
785 our linear-interpolated soil map, thus reducing the model's ability to accurately predict the
786 relationship in boreal ecosystems on a global scale. With most soil observations located around
787 the middle latitudes, it would not be surprising that our model has the greatest confidence there.
788

789 4.2 Anthropogenic Perturbation and Implications for C Cycling

790 Our model and observations suggest that anthropogenic perturbations played an important role in
791 global atmospheric Mn cycling, for which 32% of the total emissions were attributed to
792 anthropogenic sources. As the dominant contributor of emissions in most industrialized regions,
793 the influence of anthropogenic sources could be equal to or exceed that of natural sources,
794 especially in the northern hemisphere (Figure 7), where they significantly accelerated the Mn
795 turnover times in surficial soils by enriching the atmospheric deposition in which the Mn-to-N
796 ratio was boosted. Human activities, including industrialization and agricultural practices, likely
797 alter Mn cycles by a factor of two or more in many associated areas (Figure 6), on the same order
798 of magnitude as the perturbation to the cycling of other metals such as Mo, aluminum (Al), lead
799 (Pb), mercury (Hg), and vanadium (V) (Rauch & Pacyna, 2009; Schlesinger et al., 2017; Selin,
800 2009; Sen & Peucker-Ehrenbrink, 2012; Wong et al., 2021).
801

802 Our results reinforce the negative correlation between Mn and soil C storage in temperate and
803 boreal forests on a global scale (Kranabetter et al., 2021; Stendahl et al., 2017), indicating that
804 the Mn availability is likely a limiting factor on the soil organic matter decomposition that

805 consumed C from storage in these ecosystems. This implies that if atmospheric deposition is the
806 major source of Mn in surficial soil layers, it has the potential to facilitate oxidative C
807 decomposition by removing the limitation by Mn, and in regions that are sensitive to
808 anthropogenic activities, humans might indirectly alter the C cycle by releasing aerosols
809 composed of Mn into the atmosphere through industrial and agricultural activities. While a
810 significant proportion of global C is stocked in the soils and vegetation of boreal and temperate
811 forests in combination (IPCC, 2000), increased C emissions in these systems from
812 decomposition promoted by Mn addition could be important to global C dynamics and climate
813 feedbacks, exacerbating the ongoing escalating C emissions in boreal forests subjected to
814 wildfires (Phillips et al., 2022; Zhao et al., 2021a).

815
816 However, to quantitatively characterize the extent of the Mn deposition's influence on C cycling,
817 more field measurements and experimental studies are required. For example, our current
818 understanding would be improved if soil organic matters at different stages of decomposition
819 could be distinguished. Berg et al. (2007) points out that Mn addition has a stronger effect on
820 late-stage decomposition by enhancing lignin-degrading enzymes because microbes tend to
821 decompose lignin after the more labile organic substrates (Berg, 2014; Berg & Matzner, 1997).
822 In addition, we focused on modelling the total extractable and/or acid digested Mn in soils and
823 atmospheric deposition and did not consider Mn bioavailability explicitly, which is crucial to the
824 microorganisms that are responsible for decomposition and can be regulated by the cycling of
825 Mn in different oxidation states (Keiluweit et al., 2015). Incorporation of mechanisms
826 constraining the bioavailability, mobility, and reactivity of Mn (Keiluweit et al., 2015) in future
827 model calibrations is essential for a more accurate interpretation. Finally, our estimated "pseudo"
828 turnover time and the Mn-to-N ratio could only partially represent the Mn status in soils because
829 we did not include fluxes from other reservoirs in the Mn cycle. For instance, release of Mn(II)
830 from clay mineral weathering and Mn(III, IV)-oxide reduction (Canfield et al., 2005) could
831 increase the available Mn concentration in soils, creating the gap between the Mn-to-N ratio in
832 deposition and in soils.

833

834 4.3 Limitations of the Observational Data

835 Our collected atmospheric observations of Mn are spread over 6 out of 7 continents, but high
836 spatial coverage is mostly restricted to industrialized countries. To improve our understanding of
837 atmospheric contribution to the Mn cycle, more observations of the concentration and deposition
838 in currently less-observed areas such as the polar regions are needed to further constrain the
839 tuning of the model.

840

841 There are more locations with soil Mn measurements than atmospheric observations, but they
842 are concentrated mostly in Europe and the U.S. Because of the uneven distribution of the soil
843 observations and the limited number of them across many countries, we are not able to capture
844 the variability of the soil Mn concentration at small scale. For example, we did not include

845 measurements of Mn concentration at metal-contaminated sites associated with mining or other
846 industries (Lv et al., 2022) in either interpolation approach. With the currently available soil data,
847 the linear interpolation approach is uncertain in areas where in-situ soil observations are sparse
848 and less representative, whereas the problem with soil order extrapolation is that several soil
849 orders show a lack of sufficient measurements to calibrate the median value. While we gained a
850 better estimation of the dust emission scheme with a soil order extrapolation in our specific case,
851 many studies (Baize, 2010; Wong et al., 2018; Okin et al., 2008) have shown that suggested that
852 soil orders, which are the highest level of taxonomic classification, are typically inadequate when
853 dealing with trace element concentrations in soils, and the intra-order variation could be large.
854 Better estimation might be achieved with more refined classification at lower taxonomic levels
855 such as suborders and great groups, or even quantitatively with particle size distribution.
856 However, fewer sites specify the abovementioned information, and at such levels, the conversion
857 between different classification systems is more complex.

858

859 **5 Conclusions**

860 In this study, we present, for the first time, a spatially explicit estimation of the global
861 atmospheric Mn sources, distribution, and deposition using a combined model-observation
862 approach. We estimate that anthropogenic sources ($390 \text{ Gg Mn yr}^{-1}$) represent approximately 32%
863 of the total atmospheric Mn budget ($1500 \text{ Gg Mn yr}^{-1}$). Including this portion of Mn emissions in
864 the model enhanced Mn deposition in many industrialized regions, which could accelerate soil
865 Mn turnover as high as 100-fold and boost the Mn-to-N ratio in atmospheric deposition.
866 Deposition of the anthropogenic Mn from human activities have a high potential to facilitate
867 SOM decomposition in temperate and (sub)tropical forest ecosystems, thus influencing C storage
868 and the global C cycle. Given the sparsity of observations and limited understanding of
869 atmospheric Mn sources, uncertainties are high in these estimations. We need more atmospheric
870 and soil observations across different landscapes to refine our model in the future and thus
871 quantification of the global Mn cycle.

872 **Acknowledgments**

873 NMM and LL would like to acknowledge the support of DOE grant: DE-SC0021302. SR
874 acknowledges the support of grants AEROEXTREME PID2021-125669NB-I00, AEROATLAN
875 CGL 2015-66299-P & POLLINDUST CGL2011-26259 funded by ERDF and the Research State
876 Agency of Spain.

877

878 **Data Availability Statement**

879 Observational synthesis available in the supplemental materials, while model results are
880 available at the Cornell eCommons repository.

881

882 **References**

- 883 Abanda, P. A., Compton, J. S., & Hannigan, R. E. (2011). Soil nutrient content, above-ground
884 biomass and litter in a semi-arid shrubland, South Africa. *Geoderma*, *164*(3–4), 128–137.
885 <https://doi.org/10.1016/j.geoderma.2011.05.015>
- 886 Adebisi, A., Kok, J. F., Murray, B. J., Ryder, C. L., Stuut, J.-B. W., Kahn, R. A., Knippertz, P.,
887 Formenti, P., Mahowald, N. M., Pérez García-Pando, C., Klose, M., Ansmann, A., Samset, B.
888 H., Ito, A., Balkanski, Y., Di Biagio, C., Romanias, M. N., Huang, Y., & Meng, J. (2023). A
889 review of coarse mineral dust in the Earth system. *Aeolian Research*, *60*, 100849.
890 <https://doi.org/10.1016/j.aeolia.2022.100849>
- 891 Albani, S., Mahowald, N. M., Perry, A. T., Scanza, R. A., Zender, C. S., Heavens, N. G., Maggi,
892 V., Kok, J. F., & Otto-Bliesner, B. L. (2014). *Journal of Advances in Modelling Earth Systems*,
893 *6*(3), 541-570. <https://doi.org/10.1002/2013MS000279>
- 894 Alfaro, M. R., Montero, A., Ugarte, M. O., do Nascimento, C. W. A., de Aguiar Accioly, A. M.,
895 Biondi, C. M., & da Silva, Y. J. (2015). Background concentrations and reference values for
896 heavy metals in soils of Cuba. *Environmental Monitoring and Assessment*, *187*(1).
897 <https://doi.org/10.1007/s10661-014-4198-3>
- 898 Alongi, D. M., Wattayakorn, G., Boyle, S., Tirendi, F., & Payn C and Dixon, P. (2004).
899 Influence of roots and climate on mineral and trace element storage and flux in tropical
900 mangrove soils. *Biogeochemistry* *69*(1), 105–123.
901 <https://doi.org/10.1023/B:BIOG.0000031043.06245.af>
- 902 Alves, C., Gonçalves, C., Fernandes, A. P., Tarelho, L., & Pio, C. (2011). Fireplace and
903 woodstove fine particle emissions from combustion of western Mediterranean wood types.
904 *Atmospheric Research*, *101*(3), 692–700. <https://doi.org/10.1016/j.atmosres.2011.04.015>

- 905 Andela, N., Morton, D. C., Giglio, L., Chen, Y., van der Werf, G. R., Kasibhatla, P. S., DeFries,
906 R. S., Collatz, G. J., Hantson, S., Kloster, S., Bachelet, D., Forrest, M., Lasslop, G., Li, F.,
907 Mangeon, S., Melton, J. R., Yue, C., & Randerson, J. T. (2017). A human-driven decline in
908 global burned area. *Science*, *356*(6345), 1356–1362. <https://doi.org/10.1126/science.aal4108>
- 909 Andruszczak, E. (1975). Zawartość makro- i mikroelementów w glebach i roślinności użytków
910 rolnych Kotliny Kłodzkiej. *Roczniki Gleboznawcze*, *26*(3).
- 911 Arditoglou, A., Petaloti, C., Terzi, E., Sofoniou, M., & Samara, C. (2004). Size distribution of
912 trace elements and polycyclic aromatic hydrocarbons in fly ashes generated in Greek lignite-fired
913 power plants. *The Science of the Total Environment*, *323*, 153–167.
914 <https://doi.org/10.1016/j.scitotenv.2003.10.013>
- 915 Asawalam, D. O., & Johnson, S. (2007). Physical and chemical characteristics of soils modified
916 by earthworms and termites. *Communications in Soil Science and Plant Analysis*, *38*(3–4), 513–
917 521. <https://doi.org/10.1080/00103620601174569>
- 918 Baize, D. (2010). *Concentrations of trace elements in soils: The three keys*. IUSS-International
919 Union of Soil Sciences. <https://www.researchgate.net/publication/275645543>
- 920 Batjes, N. H. (1997). A world data set of derived soil properties by FAO-UNESCO soil unit for
921 global modelling. *Soil Use and Management*, *13*, pp. 9-16.
- 922 Becquer, T., Quantin, C., & Boudot, J. P. (2010). Toxic levels of metals in Ferralsols under
923 natural vegetation and crops in New Caledonia. *European Journal of Soil Science*, *61*(6), 994–
924 1004. <https://doi.org/10.1111/j.1365-2389.2010.01294.x>
- 925 Berg, B. (2014). Decomposition patterns for foliar litter – A theory for influencing factors. *Soil*
926 *Biology and Biochemistry*, *78*, 222–232. <https://doi.org/10.1016/j.soilbio.2014.08.005>

- 927 Berg, B., Davey, M. P., de Marco, A., Emmett, B., Faituri, M., Hobbie, S. E., Johansson, M. B.,
928 Liu, C., McClaugherty, C., Norell, L., Rutigliano, F. A., Vesterdal, L., & Virzo De Santo, A.
929 (2010). Factors influencing limit values for pine needle litter decomposition: A synthesis for
930 boreal and temperate pine forest systems. *Biogeochemistry*, *100*(1), 57–73.
931 <https://doi.org/10.1007/s10533-009-9404-y>
- 932 Berg, B. (2000). Litter decomposition and organic matter turnover in northern forest soils. *Forest*
933 *Ecology and Management*, *133*(1-2), 13-22. [https://doi.org/10.1016/S0378-1127\(99\)00294-7](https://doi.org/10.1016/S0378-1127(99)00294-7)
- 934 Berg, B., & Matzner, E. (1997). Effect of N deposition on decomposition of plant litter and soil
935 organic matter in forest systems. *Environmental Reviews*, *5*(1), 1–25.
936 <https://doi.org/10.1139/a96-017>
- 937 Berg, B., Steffen, K. T., & McClaugherty, C. (2007). Litter decomposition rate is dependent on
938 litter Mn concentrations. *Biogeochemistry*, *82*(1), 29–39. [https://doi.org/10.1007/s10533-006-](https://doi.org/10.1007/s10533-006-9050-6)
939 [9050-6](https://doi.org/10.1007/s10533-006-9050-6)
- 940 Beygi, M., & Jalali, M. (2018). Background levels of some trace elements in calcareous soils of
941 the Hamedan Province, Iran. *Catena*, *162*, 303–316.
942 <https://doi.org/https://doi.org/10.1016/j.catena.2017.11.001>
- 943 Bibak, A., Moberg, J. P., & Borggaard, O. K. (1994). Content and distribution of cobalt, copper,
944 manganese and molybdenum in Danish spodosols and ultisols. *Acta Agriculturae Scandinavica*,
945 *Section B — Soil & Plant Science*, *44*(4), 208–213. <https://doi.org/10.1080/09064719409410247>
- 946 Block, C., & Dams, R. (1976). Study of fly ash emission during combustion of coal.
947 *Environmental Science & Technology*, *10*(10), 1011–1017. <https://doi.org/10.1021/es60121a013>

- 948 Boente, C., Matanzas, N., García-González, N., Rodríguez-Valdés, E., & Gallego, J. R. (2017).
949 Trace elements of concern affecting urban agriculture in industrialized areas: A multivariate
950 approach. *Chemosphere*, *183*, 546–556. <https://doi.org/10.1016/j.chemosphere.2017.05.129>
- 951 Bond, T. C., Streets, D. G., Yarber, K. F., Nelson, S. M., Woo, J. H., & Klimont, Z. (2004). A
952 technology-based global inventory of black and organic carbon emissions from combustion.
953 *Journal of Geophysical Research: Atmospheres*, *109*(14). <https://doi.org/10.1029/2003JD003697>
- 954 Boucher, O., D. Randall, P. Artaxo, C. Bretherton, G. Feingold, P. Forster, V.-M. Kerminen, Y.
955 Kondo, H. Liao, U. Lohmann, P. Rasch, S.K. Satheesh, S. Sherwood, B. Stevens, & Zhang X. Y.
956 (2013). Clouds and aerosols. In T.F. Stocker, D. Qin, G.-K. Plattner, M. Tignor, S.K. Allen, J.
957 Doschung, A. Nauels, Y. Xia, V. Bex, and P.M. Midgley (Eds.), *Climate Change 2013: The*
958 *Physical Science Basis. Contribution of Working Group I to the Fifth Assessment Report of the*
959 *Intergovernmental Panel on Climate Change* (pp. 571-657). Cambridge University Press.
960 <https://doi.org/10.1017/CBO9781107415324.016>.
- 961 Bradford, G. R., Chang, A. C., Page, A. L., Bakhtar, D., Frampton, J. A., & Wright, H. (1996).
962 *Kearney foundation special report: Background Concentrations of Trace and Major Elements in*
963 *California Soils*. Kearney Foundation of Soil Science, Division of Agriculture and Natural
964 Resources, University of California.
- 965 Brahney, J., Mahowald, N., Ward, D. S., Ballantyne, A. P., & Neff, J. C. (2015). Is atmospheric
966 phosphorus pollution altering global alpine Lake stoichiometry? *Global Biogeochemical Cycles*,
967 *29*(9), 1369–1383. <https://doi.org/10.1002/2015GB005137>
- 968 Browning, T. J., Achterberg, E. P., Engel, A., & Mawji, E. (2021). Manganese co-limitation of
969 phytoplankton growth and major nutrient drawdown in the Southern Ocean. *Nature*
970 *Communications*, *12*(1), 884. <https://doi.org/10.1038/s41467-021-21122-6>

- 971 Buccolieri, A., Buccolieri, G., Dell'Atti, A., Strisciullo, G., & Gagliano-Candela, R. (2010).
972 Monitoring of total and bioavailable heavy metals concentration in agricultural soils.
973 *Environmental Monitoring and Assessment*, 168(1), 547–560. [https://doi.org/10.1007/s10661-](https://doi.org/10.1007/s10661-009-1133-0)
974 009-1133-0
- 975 Bullard, J., Baddock, M., McTainsh, G., & Leys, J. (2008). Sub-basin scale dust source
976 geomorphology detected using MODIS. *Geophysical Research Letters*, 35(15), L15404.
977 <https://doi.org/10.1029/2008GL033928>
- 978 Burrows, S. M., Elbert, W., Lawrence, M. G., & Poschl, U. (2009). Bacteria in the global
979 atmosphere--Part 1: Review and synthesis of literature for different ecosystems. *Atmospheric*
980 *Chemistry and Physics*, 9, 9263–9280.
- 981 Burt, R., Weber, T., Park, S., Yochum, S., & Ferguson, R. (2011). Trace Element Concentration
982 and Speciation in Selected Mining-Contaminated Soils and Water in Willow Creek Floodplain,
983 Colorado. *Applied and Environmental Soil Science*, 2011, 237071.
984 <https://doi.org/10.1155/2011/237071>
- 985 Cabrera, F., Clemente, L., Barrientos, E. D., Lopez, R., & Murillo, J. (1999). Heavy metal
986 pollution of soils affected by the Guadiamar toxic flood. *Science of the Total Environemnt*,
987 242(1–3), 117–129. [https://doi.org/10.1016/S0048-9697\(99\)00379-4](https://doi.org/10.1016/S0048-9697(99)00379-4)
- 988 Cancela, R. C., de Abreu, C. A., & Paz-Gonzalez, A. (2002). DTPA and Mehlich-3
989 micronutrient extractability in natural soils. *Communications in Soil Science and Plant Analysis*,
990 33(15–18), 2879–2893. <https://doi.org/10.1081/CSS-120014488>
- 991 Canfield, D. E., Kristensen, E., & Thamdrup, B. (2005). The Iron and Manganese Cycles. In
992 *Advances in Marine Biology*, 48 (pp. 269–312). Elsevier. [https://doi.org/10.1016/S0065-](https://doi.org/10.1016/S0065-2881(05)48008-6)
993 2881(05)48008-6

994 Cassol, J. C., Pletsch, A. L., Costa Júnior, I. L., Bocardi, J., Alovissil, A. M. T., & Fronza, F. L.
995 (2020). Natural contents of metals in soils from basaltic origins in western Parana, Brazil.
996 *Revista Brasileira de Ciências Agrárias*, 15(2). <https://doi.org/10.5039/agraria.v15i2a6992>

997 Cavallari, J. M., Eisen, E. A., Fang, S. C., Schwartz, J., Hauser, R., Herrick, R. F., & Christiani,
998 D. C. (2008). PM_{2.5} metal exposures and nocturnal heart rate variability: A panel study of
999 boilermaker construction workers. *Environmental Health: A Global Access Science Source*, 7.
1000 <https://doi.org/10.1186/1476-069X-7-36>

1001 Chen, J. S., Wei, F. S., Zheng, C. J., Wu, Y. Y., & Adriano, D. C. (1991). Background
1002 concentrations of elements in soils of China. *Water Air and Soil Pollution*, 57(8), 699–712.
1003 <https://doi.org/10.1007/BF00282934>

1004 Chen, M., Ma, L. Q., & Harris, W. G. (1999). Baseline concentrations of 15 trace elements in
1005 Florida surface soils. *Journal of Environmental Quality*, 28(4), 1173–1181.
1006 <https://doi.org/10.2134/jeq1999.00472425002800040018x>

1007 Chen, M., Ma, L. Q., & Li, Y. C. (2000). Concentrations of P, K, Al, Fe, Mn, Cu, Zn, and As in
1008 marl soils from south Florida. *Annual Proceedings Soil and Crop Science Society of Florida*, 59,
1009 124–129.

1010 China, S., Veghte, D., Ahkami, A. H., Weis, J., Jansson, C., Guenther, A. B., Gilles, M. K., &
1011 Laskin, A. (2020). Microanalysis of Primary Biological Particles from Model Grass over Its Life
1012 Cycle. *ACS Earth and Space Chemistry*, 4(10), 1895–1905.
1013 <https://doi.org/10.1021/acsearthspacechem.0c00144>

1014 Computational and Information Systems Laboratory (2019). Cheyenne: HPE/SGI ICE XA
1015 System (NCAR Community Computing). Boulder, CO: National Center for Atmospheric
1016 Research. Retrieved from <https://doi.org/10.5065/D6RX99HX>

1017 Córdoba, P., Ochoa-Gonzalez, R., Font, O., Izquierdo, M., Querol, X., Leiva, C., López-Antón,
1018 M. A., Díaz-Somoano, M., Rosa Martínez-Tarazona, M., Fernandez, C., & Tomás, A. (2012).
1019 Partitioning of trace inorganic elements in a coal-fired power plant equipped with a wet Flue Gas
1020 Desulphurisation system. *Fuel*, 92(1), 145–157. <https://doi.org/10.1016/j.fuel.2011.07.025>
1021 da Silva Costa, R. D., Paula Neto, P., Costa Campos, M. C., do Nascimento, W. B., do
1022 Nascimento, C. W., Silva, L. S., & da Cunha, J. M. (2017). Natural contents of heavy metals in
1023 soils of the southern Amazonas state, Brazil. *Semina-Ciencias Agrarias*, 38(6), 3499–3513.
1024 <https://doi.org/10.5433/1679-0359.2017v38n6p3499>
1025 da Silva, Y. J. A. B., do Nascimento, C. W. A., Cantalice, J. R. B., da Silva, Y. J. A. B., & Cruz,
1026 C. M. C. A. (2015). Watershed-scale assessment of background concentrations and guidance
1027 values for heavy metals in soils from a semiarid and coastal zone of Brazil. *Environmental*
1028 *Monitoring and Assessment*, 187(9), 558. <https://doi.org/10.1007/s10661-015-4782-1>
1029 Dantu, S. (2010a). Factor analysis applied to a geochemical study of soils from parts of Medak
1030 and Sangareddy areas, Medak district, Andhra Pradesh, India. *Environmental Monitoring and*
1031 *Assessment*, 162(1–4), 139–152. <https://doi.org/10.1007/s10661-009-0782-3>
1032 Dantu, S. (2010b). Geochemical patterns in soils in and around Siddipet, Medak District, Andhra
1033 Pradesh, India. *Environmental Monitoring and Assessment*, 170(1–4), 681–701.
1034 <https://doi.org/10.1007/s10661-009-1267-0>
1035 Darwish, M. A. G., & Poellmann, H. (2015). Trace elements assessment in agricultural and
1036 desert soils of Aswan area, south Egypt: Geochemical characteristics and environmental impacts.
1037 *Journal of African Earth Sciences*, 112(A), 358–373.
1038 <https://doi.org/10.1016/j.jafrearsci.2015.06.018>

- 1039 Davey, M. P., Berg, B., Emmett, B. A., & Rowland, P. (2007). Decomposition of oak leaf litter
1040 is related to initial litter Mn concentrations. *Canadian Journal of Botany*, 85(1), 16–24.
1041 <https://doi.org/10.1139/b06-150>
- 1042 Davies-Barnard, T., & Friedlingstein, P. (2020). The Global Distribution of Biological Nitrogen
1043 Fixation in Terrestrial Natural Ecosystems. *Global Biogeochemical Cycles*, 34(3).
1044 <https://doi.org/10.1029/2019GB006387>
- 1045 Davison, R. L., Natusch, D. F. S., Wallace, J. R., & Evans, C. A. (1974). Trace elements in fly
1046 ash. Dependence of concentration on particle size. *Environmental Science & Technology*, 8(13),
1047 1107–1113. <https://doi.org/10.1021/es60098a003>
- 1048 de Souza, C. A. C. de, Machado, A. T., Lima, L. R. P. de A., & Cardoso, R. J. C. (2010).
1049 Stabilization of electric-arc furnace dust in concrete. *Materials Research*, 13(4), 513–519.
1050 <https://doi.org/10.1590/S1516-14392010000400014>
- 1051 de Souza, J. J., Pereira Abrahao, W. A., de Mello, J. W., da Silva, J., da Costa, L. M., & de
1052 Oliveira, T. S. (2015). Geochemistry and spatial variability of metal(loid) concentrations in soils
1053 of the state of Minas Gerais, Brazil. *Science of the Total Environment*, 505, 338–349.
1054 <https://doi.org/10.1016/j.scitotenv.2014.09.098>
- 1055 Dentener, F., Drevet, J., Lamarque, J. F., Bey, I., Eickhout, B., Fiore, A. M., Hauglustaine, D.,
1056 Horowitz, L. W., Krol, M., Kulshrestha, U. C., Lawrence, M., Galy-Lacaux, C., Rast, S.,
1057 Shindell, D., Stevenson, D., Van Noije, T., Atherton, C., Bell, N., Bergman, D., . . . Wild, O.
1058 (2006). Nitrogen and sulfur deposition on regional and global scales: A multimodel evaluation.
1059 *Global Biogeochemical Cycles*, 20(4). <https://doi.org/10.1029/2005GB002672>

1060 Desboeufs, K. v., Sofikitis, A., Losno, R., Colin, J. L., & Ausset, P. (2005). Dissolution and
1061 solubility of trace metals from natural and anthropogenic aerosol particulate matter.
1062 *Chemosphere*, 58(2), 195–203. <https://doi.org/10.1016/j.chemosphere.2004.02.025>

1063 Després, VivianeR., Huffman, J. A., Burrows, S. M., Hoose, C., Safatov, AleksandrS., Buryak,
1064 G., Fröhlich-Nowoisky, J., Elbert, W., Andreae, MeinratO., Pöschl, U., & Jaenicke, R. (2012).
1065 Primary biological aerosol particles in the atmosphere: a review. *Tellus B: Chemical and*
1066 *Physical Meteorology*, 64(1), 15598. <https://doi.org/10.3402/tellusb.v64i0.15598>

1067 do Nascimento, C. W., Vieira Lima Luiz Henrique and da Silva, F. L., Biondi, C. M., & Costa
1068 Campos, M. C. (2018). Natural concentrations and reference values of heavy metals in
1069 sedimentary soils in the Brazilian Amazon. *Environmental Monitoring and Assessment*, 190(10).
1070 <https://doi.org/10.1007/s10661-018-6989-4>

1071 Dolan, R., Vanloon, J., Templeton, D., & Paudyn, A. (1990). Assessment of ICP-MS for routine
1072 multielement analysis of soil samples in environmental trace-element studies. *Fresenius Journal*
1073 *of Analytical Chemistry*, 336(2), 99–105. <https://doi.org/10.1007/BF00322545>

1074 Dreher, K. L., Jaskot, R. H., Lehmann, J. R., Richards, J. H., McGee, J. K., Ghio, A. J., & Costa,
1075 D. L. (1997). Soluble transition metals mediate residual oil fly ash induced acute lung injury.
1076 *Journal of Toxicology and Environmental Health*, 50(3), 285–305.
1077 <https://doi.org/10.1080/009841097160492>

1078 Expósito, A., Markiv, B., Ruiz-Azcona, L., Santibáñez, M., & Fernández-Olmo, I. (2021).
1079 Personal inhalation exposure to manganese and other trace metals in an environmentally exposed
1080 population: Bioaccessibility in size-segregated particulate matter samples. *Atmospheric Pollution*
1081 *Research*, 12(8). <https://doi.org/10.1016/j.apr.2021.101123>

1082 Fernandes, A. R., de Souza, E. S., de Souza Braz, A. M., Birani, S. M., & Alleoni, L. R. F.
1083 (2018). Quality reference values and background concentrations of potentially toxic elements in
1084 soils from the Eastern Amazon, Brazil. *Journal of Geochemical Exploration*, *190*, 453–463.
1085 <https://doi.org/10.1016/j.gexplo.2018.04.012>

1086 Foulds, W. (1993). Nutrient concentrations of Foliage and soil in south-western Australia. *New*
1087 *Phytologist*, *125*(3), 529–546. <https://doi.org/10.1111/j.1469-8137.1993.tb03901.x>

1088 Franklin, R. E., Duis, L., Smith, B. R., Brown, R., & Toler, J. E. (2003). Elemental
1089 concentrations in soils of South Carolina. *Soil Science*, *168*(4), 280–291.
1090 <https://doi.org/10.1097/00010694-200304000-00005>

1091 Frey, S. D., Ollinger, S., Nadelhoffer, K., Bowden, R., Brzostek, E., Burton, A., Caldwell, B. A.,
1092 Crow, S., Goodale, C. L., Grandy, A. S., Finzi, A., Kramer, M. G., Lajtha, K., LeMoine, J.,
1093 Martin, M., McDowell, W. H., Minocha, R., Sadowsky, J. J., Templer, P. H., & Wickings, K.
1094 (2014). Chronic nitrogen additions suppress decomposition and sequester soil carbon in
1095 temperate forests. *Biogeochemistry*, *121*(2), 305–316. [https://doi.org/10.1007/s10533-014-0004-](https://doi.org/10.1007/s10533-014-0004-0)
1096 [0](https://doi.org/10.1007/s10533-014-0004-0)

1097 Galloway, J. N., Winiwarter, W., Leip, A., Leach, A. M., Bleeker, A., & Erisman, J. W. (2014).
1098 Nitrogen footprints: past, present and future. *Environmental Research Letters*, *9*(11).
1099 <https://doi.org/https://doi.org/10.1088/1748-9326/9/11/115003>

1100 Gelaro, R., McCarty, W., Suárez, M. J., Todling, R., Molod, A., Takacs, L., Randles, C.,
1101 Darnenov, A., Bosilovich, M. G., Reichle, R., Wargan, K., Coy, L., Cullather, R., Draper, C.,
1102 Akella, S., Buchard, V., Conaty, A., da Silva, A., Gu, W., . . . & Zhao, B. (2017). The modern-
1103 era retrospective analysis for research and applications, version 2 (MERRA-2). *Journal of*
1104 *Climate*, *30*(13), 5419–5454. <https://doi.org/10.1175/JCLI-D-16-0758.1>

- 1105 Ghaemi, Z., Karbassi, A. R., Moattar, F., Hassani, A., & Khorasani, N. (2015). Evaluating soil
1106 metallic pollution and consequent human health hazards in the vicinity of an industrialized zone,
1107 case study of Mubarakeh steel complex, Iran. *Journal of Environmental Health Science and*
1108 *Engineering*, *13*. <https://doi.org/10.1186/s40201-015-0231-x>
- 1109 Ginoux, P., Prospero, J., Gill, T. E., Hsu, N. C., & Zhao, M. (2012). Global scale attribution of
1110 anthropogenic and natural dust sources and their emission rates based on MODIS deep blue
1111 aerosol products. *Reviews of Geophysics*, *50*(RG3005). <https://doi.org/10.1029/2012RG000388>
- 1112 Hamilton, D. S., Perron, M. M. G., Bond, T. C., Bowie, A. R., Buchholz, R. R., Guieu, C., Ito,
1113 A., Maenhaut, W., Myriokefalitakis, S., Olgun, N., Rathod, S. D., Schepanski, K., Tagliabue, A.,
1114 Wagner, R., & Mahowald, N. M. (2022). Earth, Wind, Fire, and Pollution: Aerosol Nutrient
1115 Sources and Impacts on Ocean Biogeochemistry. *Annual Review of Marine Science*, *14*(1), 303–
1116 330. <https://doi.org/10.1146/annurev-marine-031921-013612>
- 1117 Hand, J. L., Gill, T. E., & Schichtel, B. A. (2017). Spatial and seasonal variability in fine mineral
1118 dust and coarse aerosol mass at remote sites across the United States. *Journal of Geophysical*
1119 *Research*, *122*(5), 3080–3097. <https://doi.org/10.1002/2016JD026290>
- 1120 Hand, J. L., Gill, T. E., & Schichtel, B. A. (2019). Urban and rural coarse aerosol mass across the
1121 United States: Spatial and seasonal variability and long-term trends. *Atmospheric Environment*,
1122 *218*. <https://doi.org/10.1016/j.atmosenv.2019.117025>
- 1123 Hansen, H. K., Pedersen, A. J., Ottosen, L. M., & Villumsen, A. (2001). Speciation and mobility
1124 of cadmium in straw and wood combustion fly ash. *Chemosphere*, *45*(1), 123–128.
1125 [https://doi.org/10.1016/S0045-6535\(01\)00026-1](https://doi.org/10.1016/S0045-6535(01)00026-1)
- 1126 Hansen, M. C., Potapov, P. v, Moore, R., Hancher, M., Turubanova, S. A., Tyukavina, A., Thau,
1127 D., Stehman, S. v, Goetz, S. J., Loveland, T. R., Kommareddy, A., Egorov, A., Chini, L., Justice,

- 1128 C. O., & Townshend, J. R. G. (2013). High-Resolution Global Maps of 21st-Century Forest
1129 Cover Change. *Science*, *342*(6160), 850–853. <https://doi.org/10.1126/science.1244693>
- 1130 Hartley, I. P., Hill, T. C., Chadburn, S. E., & Hugelius, G. (2021). Temperature effects on carbon
1131 storage are controlled by soil stabilisation capacities. *Nature Communications*, *12*(1), 6713.
1132 <https://doi.org/10.1038/s41467-021-27101-1>
- 1133 Haynes, R. J., & Swift, R. S. (1991). Concentrations of extractable Cu, Zn, Fe and Mn in a group
1134 of soils as influenced by air-drying and oven-drying and rewetting. *Geoderma*, *49*(3–4), 319–
1135 333. [https://doi.org/10.1016/0016-7061\(91\)90083-6](https://doi.org/10.1016/0016-7061(91)90083-6)
- 1136 He, Q., & Walling, D. E. (1997). The distribution of fallout ^{137}Cs and ^{210}Pb in undisturbed and
1137 cultivated soils. *Applied Radiation and Isotopes*, *48*(5), 677–690. [https://doi.org/10.1016/S0969-](https://doi.org/10.1016/S0969-8043(96)00302-8)
1138 [8043\(96\)00302-8](https://doi.org/10.1016/S0969-8043(96)00302-8)
- 1139 Heald, C., & Spracklen, D. (2009). Atmospheric budget of primary biological aerosol particles
1140 from fungal sources. *Geophysical Research Letters*, *36*(9), L09806.
1141 <https://doi.org/10.1029/2009GL037493>
- 1142 Hertel, O., Geels, C., Frohn, L. M., Ellermann, T., Skjøth, C.A., Løfstrøm, P., Christensen, J. H.,
1143 Andersen, H. V., & Peel, R. G. (2013). Assessing atmospheric nitrogen deposition to natural and
1144 semi-natural ecosystems – Experience from Danish studies using the DAMOS. *Atmospheric*
1145 *Environment*, *66*, 151-160. <https://doi.org/10.1016/j.atmosenv.2012.02.071>
- 1146 Hofrichter, M. (2002). Review: lignin conversion by manganese peroxidase (MnP). *Enzyme and*
1147 *Microbial Technology*, *30*(4), 454-466. [https://doi.org/10.1016/S0141-0229\(01\)00528-2](https://doi.org/10.1016/S0141-0229(01)00528-2)
- 1148 Hsu, C. Y., Chiang, H. C., Lin, S. L., Chen, M. J., Lin, T. Y., & Chen, Y. C. (2016). Elemental
1149 characterization and source apportionment of PM₁₀ and PM_{2.5} in the western coastal area of

1150 central Taiwan. *Science of the Total Environment*, 541, 1139–1150.
1151 <https://doi.org/10.1016/j.scitotenv.2015.09.122>

1152 Hua, Z., Chun-ming, J., Yong-gang, X., & Qiang, M. (2013). Analysis on Concentration,
1153 Distribution and Budgets of Mn and Zn in Soybean by Using ICP-AES. *Spectroscopy and*
1154 *Spectral Analysis*, 33(4), 1112–1115. [https://doi.org/10.3964/j.issn.1000-0593\(2013\)04-1112-04](https://doi.org/10.3964/j.issn.1000-0593(2013)04-1112-04)

1155 Huffman, G. P., Huggins, F. E., Shah, N., Huggins, R., Linak, W. P., Miller, C. A., Pugmire, R.
1156 J., Meuzelaar, H. L. C., Seehra, M. S., & Manivannan, A. (2000). Characterization of Fine
1157 Particulate Matter Produced by Combustion of Residual Fuel Oil. *Journal of the Air & Waste*
1158 *Management Association*, 50(7), 1106–1114. <https://doi.org/10.1080/10473289.2000.10464157>

1159 Hurrell, J. W., Holland, M. M., Gent, P. R., Chan, S., Kay, J. E., Kushner, P. J., Lamarque, J.-F.,
1160 Large, W. G., Lawrence, D., Lindsay, K., Lipscomb, W. H., Long, M. C., Mahowald, N., Marsh,
1161 D. R., Neale, R. B., Rasch, P., Vavrus, S., Vertenstein, M., Bader, D., Collins, W. D., Hack, J. J.,
1162 Kiehl, J., & Marshall, S. (2013). The Community Earth System Model: A Framework for
1163 Collaborative Research. *Bulletin of the American Meteorological Society*, 94(9), 1339-1360.
1164 <https://doi.org/10.1175/BAMS-D-12-00121.1>

1165 Hurtt, G. C., Chini, L. P., Frohking, S., Betts, R. A., Feddema, J., Fischer, G., Fisk, J. P.,
1166 Hibbard, K., Houghton, R. A., Janetos, A., Jones, C. D., Kindermann, G., Kinoshita, T.,
1167 Goldewijk, K. K., Riahi, K., Shevliakova, E., Smith, S., Stehfest, E., Thomson, A., . . . Wang, Y.
1168 P. (2011). Harmonization of land-use scenarios for the period 1500-2100: 600 years of global
1169 gridded annual land-use transitions, wood harvest, and resulting secondary lands. *Climatic*
1170 *Change*, 109(1–2), 117–161. <https://doi.org/10.1007/s10584-011-0153-2>

- 1171 Ikem, A., Campbell, M., Nyirakabibi, I., & Garth, J. (2008). Baseline concentrations of trace
1172 elements in residential soils from Southeastern Missouri. *Environmental Monitoring and*
1173 *Assessment*, 140(1), 69–81. <https://doi.org/10.1007/s10661-007-9848-2>
- 1174 Imran, M., Khan, A.-H., Aziz-ul-Hassan, Kanwal, F., Mitu, L., Amir, M., & Iqbal, M. A. (2010).
1175 Evaluation of Physico-Chemical Characteristics of Soil Samples Collected from Harrapa-
1176 Sahiwal (Pakistan). *Asian Journal of Chemistry*, 22(6), 4823–4830.
- 1177 Iñigo, V., Andrades, M., Alonso-Martirena, J. I., Marín, A., & Jiménez-Ballesta, R. (2011).
1178 Multivariate Statistical and GIS-Based Approach for the Identification of Mn and Ni
1179 Concentrations and Spatial Variability in Soils of a Humid Mediterranean Environment: La
1180 Rioja, Spain. *Water, Air, & Soil Pollution*, 222(1), 271–284. <https://doi.org/10.1007/s11270-011->
1181 [0822-9](https://doi.org/10.1007/s11270-011-0822-9)
- 1182 IPCC, (2000). *Special Report on Land Use, Land-Use Change, and Forestry*. Cambridge
1183 University Press. <https://www.ipcc.ch/report/land-use-land-use-change-and-forestry>
- 1184 Ivezic, V., Singh, B. R., Almas, A. R., & Loncaric, Z. (2011). Water extractable concentrations
1185 of Fe, Mn, Ni, Co, Mo, Pb and Cd under different land uses of Danube basin in Croatia. *Acta*
1186 *Agriculturae Scandinavica, Section B — Soil & Plant Science*, 61(8), 747–759.
1187 <https://doi.org/10.1080/09064710.2011.557392>
- 1188 Jahiruddin, M., Harada, H., Hatanaka, T., & Islam, M. R. (2000). Status of trace elements in
1189 agricultural soils of Bangladesh and relationship with soil properties. *Soil Science and Plant*
1190 *Nutrition*, 46(4), 963–968. <https://doi.org/10.1080/00380768.2000.10409161>
- 1191 Jang, H. N., Seo, Y. C., Lee, J. H., Hwang, K. W., Yoo, J. I., Sok, C. H., & Kim, S. H. (2007).
1192 Formation of fine particles enriched by V and Ni from heavy oil combustion: Anthropogenic

- 1193 sources and drop-tube furnace experiments. *Atmospheric Environment*, *41*(5), 1053–1063.
1194 <https://doi.org/10.1016/j.atmosenv.2006.09.011>
- 1195 Jones, M. E., LaCroix, R. E., Zeigler, J., Ying, S. C., Nico, P. S., & Keiluweit, M. (2020).
1196 Enzymes, Manganese, or Iron? Drivers of Oxidative Organic Matter Decomposition in Soils.
1197 *Environmental Science and Technology*, *54*(21), 14114–14123.
- 1198 Joshi, D., Srivastava, P. C., Dwivedi, R., Pachauri, S. P., & Shukla, A. K. (2017). Chemical
1199 Fractions of Mn in Acidic Soils and Selection of Suitable Soil Extractants for Assessing Mn
1200 Availability to Maize (*Zea Mays* L.). *Communications in Soil Science and Plant Analysis*, *48*(8),
1201 886–897. <https://doi.org/10.1080/00103624.2017.1322601>
- 1202 Kanakidou, M., Myriokefalitakis, S., Daskalakis, N., Fanourgakis, G., Nenes, A., Baker, A. R.,
1203 Tsigaridis, K., & Mihalopoulos, N. (2016). Past, present, and future atmospheric nitrogen
1204 deposition. *Journal of the Atmospheric Sciences*, *73*(5), 2039–2047. [https://doi.org/10.1175/JAS-](https://doi.org/10.1175/JAS-D-15-0278.1)
1205 [D-15-0278.1](https://doi.org/10.1175/JAS-D-15-0278.1)
- 1206 Kassaye, Y. A., Skipperud, L., Meland, S., Dadebo, E., Einset, J., & Salbu, B. (2012). Trace
1207 element mobility and transfer to vegetation within the Ethiopian Rift Valley lake areas. *Journal*
1208 *of Environmental Monitoring*, *14*(10), 2698–2709. <https://doi.org/10.1039/c2em30271c>
- 1209 Kaste, J. M., Friedland, A. J., & Stürup, S. (2003). Using stable and radioactive isotopes to trace
1210 atmospherically deposited Pb in Montane forest soils. *Environmental Science & Technology*,
1211 *37*(16), 3560–3567. <https://doi.org/10.1021/es026372k>
- 1212 Kauffman, J., Cummings, D. L., Ward, D. E., Babbitt, R. (1995). Fire in the Brazilian Amazon:
1213 1. Biomass, nutrient pools, and losses in slashed primary forests. *Oecologia*, *104*, 397-408.
1214 <https://doi.org/10.1007/BF00341336>

- 1215 Keiluweit, M., Nico, P., Harmon, M. E., Mao, J., Pett-Ridge, J., & Kleber, M. (2015). Long-term
1216 litter decomposition controlled by manganese redox cycling. *Proceedings of the National*
1217 *Academy of Sciences of the United States of America*, *112*(38), E5253–E5260.
1218 <https://doi.org/10.1073/pnas.1508945112>
- 1219 Kellogg, C. A., & Griffin, D. W. (2006). Aerobiology and the global transport of desert dust.
1220 *Trends in Ecology and Evolution*, *21*(11), 638–644. <https://doi.org/10.1016/j.tree.2006.07.004>
- 1221 Kloss, S., Zehetner, F., Oburger, E., Buecker Jannis and Kitzler, B., Wenzel, W. W., Wimmer,
1222 B., & Soja, G. (2014). Trace element concentrations in leachates and mustard plant tissue
1223 (*Sinapis alba* L.) after biochar application to temperate soils. *Science of the Total Environment*,
1224 *481*, 498–508. <https://doi.org/10.1016/j.scitotenv.2014.02.093>
- 1225 Kok, J. F., Mahowald, N. M., Fratini, G., Gillies, J. A., Ishizuka, M., Leys, J. F., Mikami, M.,
1226 Park, M.-S., Park, S.-U., Van Pelt, R. S., & Zobeck, T. M. (2014a). An improved dust emission
1227 model – Part 1: Model description and comparison against measurements. *Atmospheric*
1228 *Chemistry and Physics*, *14*, 13023–13041. <https://doi.org/10.5194/acp14-13023-2014>.
- 1229 Kok, J. F., Albani, S., Mahowald, N. M., & Ward, D. S. (2014b). An improved dust emission
1230 model – Part 2: Evaluation in the Community Earth System Model, with implications for the use
1231 of dust source functions, *Atmospheric Chemistry and Physics*, *14*, 13043–13061.
1232 <https://doi.org/10.5194/acp-14-13043-2014>
- 1233 Koukouzas, N., Hämäläinen, J., Papanikolaou, D., Tourunen, A., & Jäntti, T. (2007).
1234 Mineralogical and elemental composition of fly ash from pilot scale fluidised bed combustion of
1235 lignite, bituminous coal, wood chips and their blends. *Fuel*, *86*(14), 2186–2193.
1236 <https://doi.org/10.1016/j.fuel.2007.03.036>

- 1237 Kranabetter, J. M., Philpott, T. J., & Dunn, D. E. (2021). Manganese limitations and the
1238 enhanced soil carbon sequestration of temperate rainforests. *Biogeochemistry*, *156*(2), 195–209.
1239 <https://doi.org/10.1007/s10533-021-00840-5>
- 1240 Krawchuk, M. A., Moritz, M. A., Parisien, M. A., Van Dorn, J., & Hayhoe, K. (2009). Global
1241 Pyrogeography: the Current and Future Distribution of Wildfire. *PLOS ONE*, *4*(4): e5102.
1242 <https://doi.org/10.1371/journal.pone.0005102>
- 1243 Kuss, J., & Kremling, K. (1999). Spatial variability of particle associated trace elements in near-
1244 surface waters of the North Atlantic (30°N/60°W to 60°N/2°W), derived by large volume
1245 sampling. *Marine Chemistry*, *68*(1-2), 71-86. [https://doi.org/10.1016/S0304-4203\(99\)00066-3](https://doi.org/10.1016/S0304-4203(99)00066-3)
- 1246 Lavado, R. S., & Porcelli, C. A. (2000). Contents and main fractions of trace elements in Typic
1247 Argiudolls of the Argentinean Pampas. *Chemical Speciation and Bioavailability*, *12*(2), 67–70.
1248 <https://doi.org/10.3184/095422900782775553>
- 1249 Lawrence, D. M., Fisher, R. A., Koven, C. D., Oleson, K. W., Swenson, S. C., Bonan, G.,
1250 Collier, N., Ghimire, B., van Kampenhout, L., Kennedy, D., Kluzek, E., Lawrence, P. J., Li, F.,
1251 Li, H., Lombardozzi, D., Riley, W. J., Sacks, W. J., Shi, M., Vertenstein, M., . . . Zeng, X.
1252 (2019). The Community Land Model Version 5: Description of New Features, Benchmarking,
1253 and Impact of Forcing Uncertainty. *Journal of Advances in Modeling Earth Systems*, *11*(12),
1254 4245–4287. <https://doi.org/10.1029/2018MS001583>
- 1255 Li, L., Mahowald, N. M., Kok, J. F., Liu, X., Wu, M., Leung, D. M., Hamilton, D. S., Emmons,
1256 L. K., Huang, Y., Sexton, N., & Wan, J. (2022). Importance of different parameterization
1257 changes for the updated dust cycle modeling in the Community Atmosphere Model (version 6.1).
1258 *Geoscientific Model Development*, *15*(22), 8181-8219. [https://doi.org/10.5194/gmd-15-8181-](https://doi.org/10.5194/gmd-15-8181-2022)
1259 2022

- 1260 Li, L., Mahowald, N., Miller, R. L., Perez Garcia-Pando, C., Klose, M., Hamilton, D. S.,
1261 Ageitos, M. G., Ginoux, P., Balkanski, Y., Green, R. O., Kalashnikova, O., Kok, J. F., Obiso, V.,
1262 Paynter, D., Thompson, D. R. (2021). Quantifying the range of the dust direct radiative effect
1263 due to source mineralogy uncertainty. *Atmospheric Chemistry and Physics Discussions*, *21*(5),
1264 3973-4005. <https://doi.org/10.5194/acp-2020-547>
- 1265 Linak, W. P., Andrew Miller, C., & Wendt, J. O. L. (2000a). Fine particle emissions from
1266 residual fuel oil combustion: Characterization and mechanisms of formation. *Proceedings of the*
1267 *Combustion Institute*, *28*(2), 2651–2658. [https://doi.org/10.1016/S0082-0784\(00\)80684-0](https://doi.org/10.1016/S0082-0784(00)80684-0)
- 1268 Linak, W. P., Miller, C. A., & Wendt, J. O. L. (2000b). Comparison of particle size distributions
1269 and elemental partitioning from the combustion of pulverized coal and residual fuel oil. *Journal*
1270 *of the Air & Waste Management Association*, *50*(8), 1532–1544.
1271 <https://doi.org/10.1080/10473289.2000.10464171>
- 1272 Lindell, L., Astrom, M., & Oberg, T. (2010). Land-use versus natural controls on soil fertility in
1273 the Subandean Amazon, Peru. *Science of the Total Environment*, *408*(4), 965–975.
1274 <https://doi.org/10.1016/j.scitotenv.2009.10.039>
- 1275 Liu, X., Easter, R. C., Ghan, S. J., Zaveri, R., Rasch, P., Shi, X., Lamarque, J.-F., Gettleman, A.,
1276 Morrison, H., Vitt, F., Conley, A., Park, S., Neale, R., Hannay, C., Ekman, A. M. L., Hess, P.,
1277 Mahowald, N. M., Collins, W., Iacoco, M. J., . . . & Mitchell, D. (2011). Toward a minimal
1278 representation of aerosol direct and indirect effects: Model description and evaluation.
1279 *Geoscientific Model Development Discussions*, *4*(4), 3485–3598. [https://doi.org/10.5194/gmdd-](https://doi.org/10.5194/gmdd-4-3485-2011)
1280 [4-3485-2011](https://doi.org/10.5194/gmdd-4-3485-2011)
- 1281 Liu, X., Ma, P. L., Wang, H., Tilmes, S., Singh, B., Easter, R. C., Ghan, S. J., & Rasch, P. J.
1282 (2016). Description and evaluation of a new four-mode version of the Modal Aerosol Module

1283 (MAM4) within version 5.3 of the Community Atmosphere Model. *Geoscientific Model*
1284 *Development*, 9(2), 505–522. <https://doi.org/10.5194/gmd-9-505-2016>

1285 Loosmore, G. A. (2003). Evaluation and development of models for resuspension of aerosols at
1286 short times after deposition. *Atmospheric Environment*, 37(5), 639-647.
1287 [https://doi.org/10.1016/S1352-2310\(02\)00902-0](https://doi.org/10.1016/S1352-2310(02)00902-0)

1288 Lv, Y., Kabanda, G., Chen, Y., Wu, C., & Li, W. (2022). Spatial distribution and ecological risk
1289 assessment of heavy metals in manganese (Mn) contaminated site. *Frontiers in Environmental*
1290 *Science*, 10. <https://doi.org/10.3389/fenvs.2022.942544>

1291 Ma, L. Q., Tan, F., & Harris, W. G. (1997). Concentrations and distributions of eleven metals in
1292 Florida soils. *Journal of Environmental Quality*, 26(3), 769.
1293 <https://www.proquest.com/scholarly-journals/concentrations-distributions-eleven->
1294 [metals/docview/197389221/se-2?accountid=10267](https://www.proquest.com/scholarly-journals/concentrations-distributions-eleven-metals/docview/197389221/se-2?accountid=10267)

1295 Machado, J., Brehm, F., Moraes, C., Santos, C., Vilela, A., & Cunha, J. (2006). Chemical,
1296 physical, structural and morphological characterization of the electric arc furnace dust. *Journal*
1297 *of Hazardous Materials*, 136(3), 953–960. <https://doi.org/10.1016/j.jhazmat.2006.01.044>

1298 Maenhaut, W., Fernández-Jiménez, M.-T., Rajta, I., & Artaxo, P. (2002). Two-year study of
1299 atmospheric aerosols in Alta Floresta, Brazil: Multielemental composition and source
1300 apportionment. *Nuclear Instruments and Methods in Physics Research*, B189, 243-248.
1301 [https://doi.org/10.1016/S0168-583X\(01\)01050-3](https://doi.org/10.1016/S0168-583X(01)01050-3)

1302 Maenhaut, W., Fernández-Jiménez, M.-T., Rajta, I., Dubtsov I, S., Meixner, F. X., Andreae, M.
1303 O., Torr, S., Hargrove, J. W., Chimanga, P., & Mlambo, J. (2000). Long-term aerosol
1304 composition measurements and source apportionment at Rukomechi, Zimbabwe. *Journal of*
1305 *Aerosol Science*, 31, Suppl. 1, S228-S229. [https://doi.org/10.1016/S0021-8502\(00\)90237-4](https://doi.org/10.1016/S0021-8502(00)90237-4)

- 1306 Maenhaut, W., Fernández-Jiménez, M.-T., & Artaxo, P. (1999). Long-term study of atmospheric
1307 aerosols in Cuiaba, Brazil : multielemental composition, sources and source apportionment.
1308 *Journal of Aerosol Science*, 30(0021–8502), S259–S260.
- 1309 Mahowald, N., Albani, S., Kok, J. F., Engelstaeder, S., Scanza, R., Ward, D. S., & Flanner, M.
1310 G. (2014). The size distribution of desert dust aerosols and its impact on the Earth system.
1311 *Aeolian Research*, 15, 53-71. <https://doi.org/10.1016/j.aeolia.2013.09.002>
- 1312 Mahowald, N. M., Artaxo, P., Baker, A. R., Jickells, T. D., Okin, G. S., Randerson, J. T., &
1313 Townsend, A. R. (2005). Impacts of biomass burning emissions and land use change on
1314 Amazonian atmospheric phosphorus cycling and deposition. *Global Biogeochemical Cycles*,
1315 19(4). <https://doi.org/10.1029/2005GB002541>
- 1316 Mahowald, N. M., Engelstaedter, S., Luo, C., Sealy, A., Artaxo, P., Benitez-Nelson, C., Bonnet,
1317 S., Chen, Y., Chuang, P. Y., Cohen, D. D., Dulac, F., Herut, B., Johansen, A. M., Kubilay, N.,
1318 Losno, R., Maenhaut, W., Paytan, A., Prospero, J. M., Shank, L. M., & Siefert, R. L. (2009).
1319 Atmospheric iron deposition: Global distribution, variability, and human perturbations. *Annual*
1320 *Review of Marine Science*, 1, 245–278. <https://doi.org/10.1146/annurev.marine.010908.163727>
- 1321 Mahowald, N. M., Hamilton, D. S., Mackey, K. R. M., Moore, J. K., Baker, A. R., Scanza, R. A.,
1322 & Zhang, Y. (2018). Aerosol trace metal leaching and impacts on marine microorganisms.
1323 *Nature Communications*, 9, 2614. <https://doi.org/10.1038/s41467-018-04970-7>
- 1324 Mamane, Y., Miller, J. L., & Dzubay, T. G. (1986). Characterization of individual fly ash
1325 particles emitted from coal- and oil-fired power plants. *Atmospheric Environment (1967)*, 20(11),
1326 2125–2135. [https://doi.org/10.1016/0004-6981\(86\)90306-9](https://doi.org/10.1016/0004-6981(86)90306-9)

- 1327 Martinez-Tarazona, M., Palacios, J. M., Martinez-Alonso, A., & Tascon, J. (1990). The
1328 characterization of organomineral components of low-rank coals. *Fuel Processing Technology*,
1329 25, 81–87. [https://doi.org/10.1016/0378-3820\(90\)90097-C](https://doi.org/10.1016/0378-3820(90)90097-C)
- 1330 Mashi, S. A., Yaro, S. A., & Haiba, A. S. (2004). Cu, Mn, Fe, and Zn levels in soils of Shika
1331 area, Nigeria. *Biomedical and Environmental Sciences*, 17(4), 426–431.
- 1332 McKenzie, R. M. (1957). The distribution of trace elements in some South Australian red-brown
1333 earths. *Australian Journal of Agricultural Research*, 8(3), 246–252.
1334 <https://doi.org/10.1071/AR9570246>
- 1335 Meij, R. (1994). Trace element behavior in coal-fired power plants. *Fuel Processing Technology*,
1336 39(1–3), 199–217. [https://doi.org/10.1016/0378-3820\(94\)90180-5](https://doi.org/10.1016/0378-3820(94)90180-5)
- 1337 Michopoulos, P., Economou, A., & Nikolis, N. (2004). Soil extractable manganese and uptake in
1338 a natural fir stand grown on calcareous soils. *Communications in Soil Science and Plant*
1339 *Analysis*, 35(1–2), 233–241. <https://doi.org/10.1081/CSS-120027646>
- 1340 Michopoulos, P., Farmaki, E., & Thomaidis, N. (2017). Foliar status and factors affecting foliar
1341 and soil chemistry in a natural aleppo pine forest. *Journal of Plant Nutrition*, 40(10), 1443–1452.
1342 <https://doi.org/10.1080/01904167.2016.1269341>
- 1343 Mikkonen, H. G., Clarke, B. O., Dasika, R., Wallis, C. J., & Reichman, S. M. (2017).
1344 Assessment of ambient background concentrations of elements in soil using combined survey
1345 and open-source data. *Science of the Total Environment*, 580, 1410–1420.
1346 <https://doi.org/10.1016/j.scitotenv.2016.12.106>
- 1347 Miko, S., Durn, G., Adamcova, R., Covic, M., Dubikova, M., Skalsky, R., Kapelj, S., & Ottner,
1348 F. (2003). Heavy metal distribution in karst soils from Croatia and Slovakia. *Environmental*
1349 *Geology*, 45(2), 262–272. <https://doi.org/10.1007/s00254-003-0878-y>

- 1350 Moore, J. A. M., Anthony, M. A., Pec, G. J., Trocha, L. K., Trzebny, A., Geyer, K. M., van
1351 Diepen, L. T. A., & Frey, S. D. (2021). Fungal community structure and function shifts with
1352 atmospheric nitrogen deposition. *Global Change Biology*, 27(7), 1349–1364.
1353 <https://doi.org/10.1111/gcb.15444>
- 1354 Moore, O. W., Curti, L., Woulds, C., Bradley, J. A., Babakhani, P., Mills, B. J. W., Homoky, W.
1355 B., Xiao, K., Bray, A. W., Fisher, B. J., Kazemian, M., Kaulich, B., Dale, A. W., & Peacock, C.
1356 L. (2023). Long-term organic carbon preservation enhanced by iron and manganese. *Nature*.
1357 <https://doi.org/10.1038/s41586-023-06325-9>
- 1358 Morales Del Mastro, A., Londonio, A., Jimenez Rebagliati, R., Pereyra, M., Dawidowski, L.,
1359 Gomez, D., & Smichowski, P. (2015). Plasma-based techniques applied to the determination of
1360 17 elements in partitioned top soils. *Microchemical Journal*, 123, 224–229.
1361 <https://doi.org/10.1016/j.microc.2015.07.002>
- 1362 Nalovic, L., & Pinta, M. (1969). Recherches sur les éléments traces dans les sols tropicaux:
1363 Étude de quelques sols de madagascar. *Geoderma*, 3, 117–132. [https://doi.org/10.1016/0016-](https://doi.org/10.1016/0016-7061(69)90008-1)
1364 [7061\(69\)90008-1](https://doi.org/10.1016/0016-7061(69)90008-1)
- 1365 Nanzyo, M., Yamasaki, S.-I., & Honna, T. (2002). Changes in content of trace and ultratrace
1366 elements with an increase in noncrystalline materials in volcanic ash soils of Japan. *Clay*
1367 *Science*, 12(1), 25–32. <https://doi.org/10.11362/jcssjclayscience1960.12.25>
- 1368 Natali, S. M., Sañudo-wilhelmy, S. A., & Lerdau, M. T. (2009). Plant and soil mediation of
1369 elevated CO₂ impacts on trace metals. *Ecosystems*, 12(5), 715–727.
1370 <https://doi.org/10.1007/s10021-009-9251-7>

- 1371 Navas, A., & Lindhorfer, H. (2005). Chemical partitioning of Fe, Mn, Zn and Cr in mountain
1372 soils of the Iberian and Pyrenean ranges (NE Spain). *Soil and Sediment Contamination: An*
1373 *International Journal*, 14(3), 249–259. <https://doi.org/10.1080/15320380590928311>
- 1374 Nguyen, B. T., Do, T. K., Tran, T. van, Dang, M. K., Dell, C. J., Luu, P. V., & Vo, Q. T. K.
1375 (2018). High soil Mn and Al, as well as low leaf P concentration, may explain for low natural
1376 rubber productivity on a tropical acid soil in Vietnam. *Journal of Plant Nutrition*, 41(7), 903–
1377 914. <https://doi.org/10.1080/01904167.2018.1431674>
- 1378 Njofang, C., Matschullat, J., Amougou, A., Tchouankoué, J. P., & Heilmeyer, H. (2009). Soil and
1379 plant composition in the Noun river catchment basin, Western Cameroon: a contribution to the
1380 development of a biogeochemical baseline. *Environmental Geology*, 56(7), 1427–1436.
1381 <https://doi.org/10.1007/s00254-008-1237-9>
- 1382 Nriagu, J. O. (1989). A global assessment of natural sources of atmospheric trace metals. *Nature*,
1383 338, 47–49.
- 1384 Nygard, T., Steinnes, E., & Royset, O. (2012). Distribution of 32 Elements in Organic Surface
1385 Soils: Contributions from Atmospheric Transport of Pollutants and Natural Sources. *Water, Air,*
1386 *& Soil Pollution*, 223(2), 699–713. <https://doi.org/10.1007/s11270-011-0895-5>
- 1387 O’Dowd, C. D., de Leeuw, G. (2007). Marine aerosol production: a review of the current
1388 knowledge. *Philosophical Transactions of the Royal Society A*, 365(1856), 1753-1774.
1389 <https://doi.org/10.1098/rsta.2007.2043>
- 1390 Okin, G. S., Mahowald, N., Chadwick, O. A., & Artaxo, P. (2004). Impact of desert dust on the
1391 biogeochemistry of phosphorus in terrestrial ecosystems. *Global Biogeochemical Cycles*, 18(2).
1392 <https://doi.org/10.1029/2003GB002145>

- 1393 Pacyna, J. M., & Pacyna, E. G. (2001). An assessment of global and regional emissions of trace
1394 metals to the atmosphere from anthropogenic sources worldwide. *Environmental Reviews*, 9(4),
1395 269–298. <https://doi.org/10.1139/a01-012>
- 1396 Papadopoulos, F., Prochaska, C., Papadopoulos, A., & Eskridge K. and Kalavrouziotis, I. (2009).
1397 Mn and Zn Micronutrients Concentrations in Acidic Soils and Source Identification Using
1398 Multivariate Statistical Methods. *Communications in Soil Science and Plant Analysis*, 40(15–
1399 16), 2357–2371. <https://doi.org/10.1080/00103620903111285>
- 1400 Papastergios, G., Filippidis, A., Fernandez-Turiel, J.-L., Gimeno, D., & Sikalidis, C. (2011).
1401 Surface Soil Geochemistry for Environmental Assessment in Kavala Area, Northern Greece.
1402 *Water, Air, & Soil Pollution*, 216(1–4), 141–152. <https://doi.org/10.1007/s11270-010-0522-x>
- 1403 Parekh, P. P. (1990). *Atmospheric Environment* (Vol. 24, Issue 2).
- 1404 Patel, K. S., Chikhlekar, S., Ramteke, S., Sahu, B. L., Dahariya, N. S., & Sharma, R. (2015).
1405 Micronutrient Status in Soil of Central India. *American Journal of Plant Sciences*, 06(19), 3025–
1406 3037. <https://doi.org/10.4236/ajps.2015.619297>
- 1407 Paye, H. de S., de Mello, J. W., Pereira Abrahao, W. A., Fernandes Filho, E. I., Pinto Dias, L. C.,
1408 Oliveira Castro, M. L., de Melo, S. B., & Franca, M. M. (2010). REFERENCE QUALITY
1409 VALUES FOR HEAVY METALS IN SOILS FROM ESPIRITO SANTO STATE, BRAZIL.
1410 *REVISTA BRASILEIRA DE CIENCIA DO SOLO*, 34(6), 2041–2051.
- 1411 Petroff, A., and Zhang, L. (2010). Development and validation of a size-resolved particle dry
1412 deposition scheme for application in aerosol transport models. *Geoscientific Model Development*,
1413 3(2), 753-769. <https://doi.org/10.5194/gmd-3-753-2010>
- 1414 Phillips, C. A., Rogers, B. M., Elder, M., Cooperdock, S., Moubarak, M., Randerson, J. T., &
1415 Frumhoff, P. C. (2022). Escalating carbon emissions from North American boreal forest

1416 wildfires and the climate mitigation potential of fire management. *Science Advances*, 8(17),
1417 eabl7161. <https://doi.org/10.1126/sciadv.abl7161>

1418 Poggio, L., de Sousa, L. M., Batjes, N. H., Heuvelink, G. B. M., Kempen, B., Ribeiro, E., and
1419 Rossiter, D.: SoilGrids 2.0 (2021). Producing soil information for the globe with quantified
1420 spatial uncertainty, *SOIL*, 7, 217–240. <https://doi.org/10.5194/soil-7-217-2021>

1421 Preda, M., & Cox, M. E. (2002). Trace metal occurrence and distribution in sediments and
1422 mangroves, Pumicestone region, southeast Queensland, Australia. *Environmental International*,
1423 28(5), 433–449. [https://doi.org/10.1016/S0160-4120\(02\)00074-0](https://doi.org/10.1016/S0160-4120(02)00074-0)

1424 Prospero, J. M., Barrett, K., Church, T., Dentener, F., Duce, R. A., Galloway, J. N., Levy, H.,
1425 Moody, J., & Quinn, P. (1996). Atmospheric deposition of nutrients to the North Atlantic Basin.
1426 *Biogeochemistry*, 35(1), 27–73. <https://doi.org/10.1007/BF02179824>

1427 Puchelt, H., Kramar, U., Cumming, G. L., Krstic, D., Nöltner, Th., Schöttle, M., & Schweikle, V.
1428 (1993). Anthropogenic Pb contamination of soils, southwest Germany. *Applied Geochemistry*, 8,
1429 71–73. [https://doi.org/10.1016/S0883-2927\(09\)80014-0](https://doi.org/10.1016/S0883-2927(09)80014-0)

1430 Querol, X., Fernández-Turiel, J., & López-Soler, A. (1995). Trace elements in coal and their
1431 behaviour during combustion in a large power station. *Fuel*, 74(3), 331–343.
1432 [https://doi.org/10.1016/0016-2361\(95\)93464-O](https://doi.org/10.1016/0016-2361(95)93464-O)

1433 Rashed, M. N. (2010). Monitoring of contaminated toxic and heavy metals, from mine tailings
1434 through age accumulation, in soil and some wild plants at Southeast Egypt. *Journal of*
1435 *Hazardous Materials*, 178(1–3), 739–746. <https://doi.org/10.1016/j.jhazmat.2010.01.147>

1436 Rathod, S. D., Hamilton, D. S., Mahowald, N. M., Klimont, Z., Corbett, J. J., & Bond, T. C.
1437 (2020). A mineralogy-based anthropogenic combustion-iron emission Inventory. *Journal of*
1438 *Geophysical Research: Atmospheres*, 125(17). <https://doi.org/10.1029/2019JD032114>

- 1439 Rauch, J. N., & Pacyna, J. M. (2009). Earth's global Ag, Al, Cr, Cu, Fe, Ni, Pb, and Zn cycles.
1440 *Global Biogeochemical Cycles*, 23(2). <https://doi.org/10.1029/2008GB003376>
- 1441 Rekasi, M., & Filep, T. (2012). Fractions and background concentrations of potentially toxic
1442 elements in Hungarian surface soils. *Environmental Monitoring and Assessment*, 184(12), 7461–
1443 7471. <https://doi.org/10.1007/s10661-011-2513-9>
- 1444 Richards, J. R., Schroder, J. L., Zhang, H., Basta, N. T., Wang, Y., & Payton, M. E. (2012).
1445 Trace Elements in Benchmark Soils of Oklahoma. *Soil Science Society of America Journal*,
1446 76(6), 2031–2040. <https://doi.org/10.2136/sssaj2012.0100>
- 1447 Ridley, D. A., Heald, C. L., & Ford, B. (2012). North African dust export and deposition: A
1448 satellite and model perspective. *Journal of Geophysical Research Atmospheres*, 117(2).
1449 <https://doi.org/10.1029/2011JD016794>
- 1450 Ridley, D. A., Heald, C. L., Kok, J. F., & Zhao, C. (2016). An observationally constrained
1451 estimate of global dust aerosol optical depth. *Atmospheric Chemistry and Physics*, 16, 15097–
1452 15117. <https://doi.org/10.5194/acp-16-15097-2016>
- 1453 Roca, N., Susana Pazos, M., & Bech, J. (2012). Background levels of potentially toxic elements
1454 in soils: A case study in Catamarca (a semiarid region in Argentina). *Catena*, 92, 55–66.
1455 <https://doi.org/10.1016/j.catena.2011.11.009>
- 1456 Roca-Perez, L., Boluda, R., & Perez-Bermudez, P. (2004). Soil-plant relationships, micronutrient
1457 contents, and cardenolide production in natural populations of *Digitalis obscura*. *Journal of Plant*
1458 *Nutrition and Soil Science*, 167(1), 79–84. <https://doi.org/10.1002/jpln.200320336>
- 1459 Roca-Perez, L., Gil, C., Cervera, M. L., Gonzalez, A., Ramos-Miras, J., Pons, V., Bech, J., &
1460 Boluda, R. (2010). Selenium and heavy metals content in some Mediterranean soils. *Journal of*
1461 *Geochemical Exploration*, 107(2, SI), 110–116. <https://doi.org/10.1016/j.gexplo.2010.08.004>

- 1462 Rodríguez, S., Calzolari, G., Chiari, M., Nava, S., García, M. I., López-Solano, J., Marrero, C.,
1463 López-Darias, J., Cuevas, E., Alonso-Pérez, S., Prats, N., Amato, F., Lucarelli, F., & Querol, X.
1464 (2020). Rapid changes of dust geochemistry in the Saharan Air Layer linked to sources and
1465 meteorology. *Atmospheric Environment*, *223*, 117186.
1466 <https://doi.org/10.1016/j.atmosenv.2019.117186>
- 1467 Rosswall, T. (1976). The internal nitrogen cycle between microorganisms, vegetation and soil.
1468 *Ecological Bulletins*, *22*, 157–167. <http://www.jstor.org/stable/20112525>
- 1469 Rusjan, D., Strlic, M., Pucko, D., Selih, V. S., & Korosec-Koruza, Z. (2006). Vineyard soil
1470 characteristics related to content of transition metals in a sub-Mediterranean winegrowing region
1471 of Slovenia. *Geoderma*, *136*(3–4), 930–936. <https://doi.org/10.1016/j.geoderma.2006.06.014>
- 1472 Ryder, C. L., Highwood, E. J., Walser, A., Seibert, P., Philipp, A., & Weinzierl, B. (2019).
1473 Coarse and giant particles are ubiquitous in Saharan dust export regions and are radiatively
1474 significant over the Sahara. *Atmospheric Chemistry and Physics*, *19*, 15353-15376.
1475 <https://doi.org/10.5194/acp-19-15353-2019>
- 1476 Saglam, C. (2017). Heavy metal concentrations in serpentine soils and plants from Kizildag
1477 National Park (Isparta) in Turkey. *Fresenius Environmental Bulletin*, *26*(6), 3995–4003.
- 1478 Sako, A., Mills, A. J., & Roychoudhury, A. N. (2009). Rare earth and trace element
1479 geochemistry of termite mounds in central and northeastern Namibia: Mechanisms for micro-
1480 nutrient accumulation. *Geoderma*, *153*(1–2), 217–230.
1481 <https://doi.org/10.1016/j.geoderma.2009.08.011>
- 1482 Salonen, V.-P., & Korkka-Niemi, K. (2007). Influence of parent sediments on the concentration
1483 of heavy metals in urban and suburban soils in Turku, Finland. *Applied Geochemistry*, *22*(5),
1484 906–918. <https://doi.org/10.1016/j.apgeochem.2007.02.003>

- 1485 Sasone, F. J., Benitez-Nelson, C. R., Resing, J. A., DeCarlo, E. H., Vink, S. M., Heath, J. A.,
1486 Huebert, B. J. (2002). Geochemistry of atmospheric aerosols generated from lava-seawater
1487 interactions. *Geophysical Research Letters*, *29*(9), 49-1-49-4.
1488 <https://doi.org/10.1029/2001GL013882>
- 1489 Scanza, R. A., Mahowald, N., Ghan, S., Zender, C. S., Kok, J. F., Liu, X., Zhang, Y., & Albani,
1490 S. (2015). Modeling dust as component minerals in the Community Atmosphere Model:
1491 Development of framework and impact on radiative forcing. *Atmospheric Chemistry and*
1492 *Physics*, *15*(1). <https://doi.org/10.5194/acp-15-537-2015>
- 1493 Schlesinger, W. H., Klein, E. M., & Vengosh, A. (2017). Global biogeochemical cycle of
1494 vanadium. *Proceedings of the National Academy of Sciences of the United States of America*,
1495 *114*(52), E11092–E11100. <https://doi.org/10.1073/pnas.1715500114>
- 1496 Schmidl, C., Marr, I. L., Caseiro, A., Kotianová, P., Berner, A., Bauer, H., Kasper-Giebl, A., &
1497 Puxbaum, H. (2008). Chemical characterisation of fine particle emissions from wood stove
1498 combustion of common woods growing in mid-European Alpine regions. *Atmospheric*
1499 *Environment*, *42*(1), 126–141. <https://doi.org/10.1016/j.atmosenv.2007.09.028>
- 1500 Schutgens, N. A. J., Gryspeerdt, E., Weigum, N., Tsyro, S., Goto, D., Schulz, M., & Stier, P.
1501 (2016). Will a perfect model agree with perfect observations? The impact of spatial sampling.
1502 *Atmospheric Chemistry and Physics*, *16*(10), 6335–6353. [https://doi.org/10.5194/acp-16-6335-](https://doi.org/10.5194/acp-16-6335-2016)
1503 2016
- 1504 Sedwick, P. N., Sholkovitz, E. R., & Church, T. M. (2007). Impact of anthropogenic combustion
1505 emissions on the fractional solubility of aerosol iron: Evidence from the Sargasso Sea.
1506 *Geochemistry, Geophysics, Geosystems*, *8*(10). <https://doi.org/10.1029/2007GC001586>

- 1507 Selin, N. E. (2009). Global biogeochemical cycling of mercury: A review. *Annual Review of*
1508 *Environment and Resources*, 34, 43–63. <https://doi.org/10.1146/annurev.envIRON.051308.084314>
- 1509 Sen, I. S., & Peucker-Ehrenbrink, B. (2012). Anthropogenic Disturbance of Element Cycles at
1510 the Earth's Surface. *Environmental Science & Technology*, 46(16), 8601–8609.
1511 <https://doi.org/10.1021/es301261x>
- 1512 Sheikh-Abdullah, S. M. (2019). Availability of Fe, Zn, Cu, and Mn in Soils of Sulaimani
1513 Governorate, Kurdistan Region, Iraq. *Soil Science*, 184(3), 87–94.
1514 <https://doi.org/10.1097/SS.0000000000000255>
- 1515 Sheppard, S. C., Grant, C. A., & Drury, C. F. (2009). Trace elements in Ontario soils - mobility,
1516 concentration profiles, and evidence of non-point-source pollution. *Canadian Journal of Soil*
1517 *Science*, 89(4), 489–499. <https://doi.org/10.4141/cjss08033>
- 1518 Sierra, C. A., Trumbore, S. E., Davidson, E. A., Vicca, S., & Janssens, I. (2015). Sensitivity of
1519 decomposition rates of soil organic matter with respect to simultaneous changes in temperature
1520 and moisture. *Journal of Advances in Modeling Earth Systems*, 7(1), 335–356.
1521 <https://doi.org/https://doi.org/10.1002/2014MS000358>
- 1522 Skordas, K., Papastergios, G., & Filippidis, A. (2013). Major and trace element contents in
1523 apples from a cultivated area of central Greece. *Environmental Monitoring and Assessment*,
1524 185(10), 8465–8471. <https://doi.org/10.1007/s10661-013-3188-1>
- 1525 Smeltzer, G. G., Langille, W. M., & MacLean, K. S. (1962). Effects of some trace elements on
1526 grass and legume production in Nova Scotia. *Canadian Journal of Plant Science*, 42(1), 46–52.
1527 <https://doi.org/10.4141/cjps62-006>

- 1528 Smith, R. D., Campbell, J. A., & Nielson, K. K. (1979). Characterization and formation of
1529 submicron particles in coal-fired plants. *Atmospheric Environment (1967)*, *13*(5), 607–617.
1530 [https://doi.org/10.1016/0004-6981\(79\)90189-6](https://doi.org/10.1016/0004-6981(79)90189-6)
- 1531 Soil Survey Staff. (2011). *Soil Survey Laboratory Information Manual Soil Survey Investigations*
1532 *Report No. 45*.
- 1533 Spiro, P. A., Jacob, D. J., & Logan, J. A. (1992). Global inventory of sulfur emissions with $1^\circ \times$
1534 1° resolution. *Journal of Geophysical Research*, *97*(D5), 6023–6036.
1535 <https://doi.org/10.1029/91JD03139>
- 1536 Stajković-Srbinović, O., Buntić, A., Rasulić, N., Kuzmanović, Đ., Dinić, Z., Delić, D., & Mrvić,
1537 V. (2018). Microorganisms in soils with elevated heavy metal concentrations in southern Serbia.
1538 *Archives of Biological Sciences*, *70*(4), 707–716.
1539 <https://www.serbiosoc.org.rs/arch/index.php/abs/article/view/2913>
- 1540 Stankovic, D., Krstic, B., Knezevic, M., Sijacic-Nikolic, M., & Bjelanovic, I. (2012).
1541 concentrations of heavy metals in soil in the area of the protected natural resource “Avala” in
1542 Belgrade. *Fresenius Environmental Bulletin*, *21*(2A), 495–502.
- 1543 Steenari, B. M., Schelander, S., & Lindqvist, O. (1999). Chemical and leaching characteristics of
1544 ash from combustion of coal, peat and wood in a 12MW CFB – a comparative study. *Fuel*,
1545 *78*(2), 249–258. [https://doi.org/10.1016/S0016-2361\(98\)00137-9](https://doi.org/10.1016/S0016-2361(98)00137-9)
- 1546 Stegemann, J. A., Roy, A., Caldwell, R. J., Schilling, P. J., & Tittsworth, R. (2000).
1547 Understanding Environmental Leachability of Electric Arc Furnace Dust. *Journal of*
1548 *Environmental Engineering*, *126*(2), 112–120. [https://doi.org/10.1061/\(ASCE\)0733-](https://doi.org/10.1061/(ASCE)0733-9372(2000)126:2(112))
1549 [9372\(2000\)126:2\(112\)](https://doi.org/10.1061/(ASCE)0733-9372(2000)126:2(112))

- 1550 Stehouwer, R. C., Hindman, J. M., & MacDonald, K. E. (2010). Nutrient and Trace Element
1551 Dynamics in Blended Topsoils Containing Spent Foundry Sand and Compost. *Journal of*
1552 *Environmental Quality*, 39(2), 587–595. <https://doi.org/10.2134/jeq2009.0172>
- 1553 Steinnes, E., Lukina, N., Nikonov, V., Aamlid, D., & Røyset, O. (2000). A gradient study of 34
1554 elements in the vicinity of a copper-nickel smelter in the Kola peninsula. *Environmental*
1555 *Monitoring and Assessment*, 60(1), 71–88. <https://doi.org/10.1023/A:1006165031985>
- 1556 Stendahl, J., Berg, B., & Lindahl, B. D. (2017). Manganese availability is negatively associated
1557 with carbon storage in northern coniferous forest humus layers. *Scientific Reports*, 7(1).
1558 <https://doi.org/10.1038/s41598-017-15801-y>
- 1559 Sterckeman, T., Douay, F., Baize, D., Fourrier, H., Proix, N., Schwartz, C., & Carignan, J.
1560 (2006a). Trace element distributions in soils developed in loess deposits from northern France.
1561 *European Journal of Soil Science*, 57(3), 392–410. <https://doi.org/10.1111/j.1365->
1562 [2389.2005.00750.x](https://doi.org/10.1111/j.1365-2389.2005.00750.x)
- 1563 Sterckeman, T., Douay, F., Baize, D., Fourrier, H., Proix, N., & Schwartz, C. (2006b). Trace
1564 elements in soils developed in sedimentary materials from Northern France. *Geoderma*, 136(3–
1565 4), 912–929. <https://doi.org/10.1016/j.geoderma.2006.06.010>
- 1566 Su, Y., & Yang, R. (2008). Background concentrations of elements in surface soils and their
1567 changes as affected by agriculture use in the desert-oasis ecotone in the middle of Heihe River
1568 Basin, North-west China. *Journal of Geochemical Exploration*, 98(3), 57–64.
1569 <https://doi.org/10.1016/j.gexplo.2007.12.001>
- 1570 Trum, F., Titeux, H., Ponette, Q., & Berg, B. (2015). Influence of manganese on decomposition
1571 of common beech (*Fagus sylvatica* L.) leaf litter during field incubation. *Biogeochemistry*,
1572 *125*(3), 349–358. <https://doi.org/10.1007/s10533-015-0129-9>

- 1573 Tsai, S.-L., & Tsai, M.-S. (1998). A study of the extraction of vanadium and nickel in oil-fired
1574 fly ash. *Resources, Conservation and Recycling*, 22(3–4), 163–176.
1575 [https://doi.org/10.1016/S0921-3449\(98\)00007-X](https://doi.org/10.1016/S0921-3449(98)00007-X)
- 1576 Tsikritzis, L. I., Ganatsios, S. S., Duliu, O. G., Kavouridis, C. v, & Sawidis, T. D. (2002). Trace
1577 elements distribution in soil in areas of lignite power plants of Western Macedonia. *Journal of*
1578 *Trace and Microprobe Techniques*, 20(2), 269–282. <https://doi.org/10.1081/TMA-120003729>
- 1579 Tume, P., Bech, J., Reverter, F., Bech, J., Longan, L., Tume, L., & Sepúlveda, B. (2011).
1580 Concentration and distribution of twelve metals in Central Catalonia surface soils. *Journal of*
1581 *Geochemical Exploration*, 109(1), 92–103.
1582 <https://doi.org/https://doi.org/10.1016/j.gexplo.2010.10.013>
- 1583 Tyler, G. (2004). Vertical distribution of major, minor, and rare elements in a Haplic Podzol.
1584 *Geoderma*, 119(3–4), 277–290. <https://doi.org/10.1016/j.geoderma.2003.08.005>
- 1585 U.S. Geological Survey. (2022). *Mineral commodity summaries 2022*.
1586 <https://doi.org/10.3133/mcs2022>
- 1587 Vance, N. C., & Entry, J. A. (2000). Soil properties important to the restoration of a Shasta red
1588 fir barrens in the Siskiyou Mountains. *Forest Ecology and Management*, 138(1–3), 427–434.
1589 [https://doi.org/10.1016/S0378-1127\(00\)00428-X](https://doi.org/10.1016/S0378-1127(00)00428-X)
- 1590 Vandebussche, S., Callewaert, S., Schepanski, K., & Mazière, M. D. (2020). North African
1591 mineral dust sources: new insights from a combined analysis based on 3D dust aerosol
1592 distributions, surface winds and ancillary soil parameters. *Atmospheric Chemistry and Physics*,
1593 20(23), 15127-15146. <https://doi.org/10.5194/acp-20-15127-2020>
- 1594 van der Werf, G. R., Randerson, J. T., Collatz, G. J., Giglio, L., Kasibhatla, P. S., Arellano, A.
1595 F., Jr., Olson, S. C. & Kasischke, E. S. (2004). Continental-Scale Partitioning of Fire Emissions

1596 During the 1997 to 2001 El Niño/La Niña Period. *Science*, 303, 73-76.
1597 <https://10.1126/science.1090753>

1598 van Diepen, L. T. A., Frey, S. D., Sthultz, C. M., Morrison, E. W., Minocha, R., Pringle, A., &
1599 Peters, D. P. C. (2015). Changes in litter quality caused by simulated nitrogen deposition
1600 reinforce the N-induced suppression of litter decay. *Ecosphere*, 6(10).
1601 <https://doi.org/10.1890/ES15-00262.1>

1602 van Marle, M. J. E., Kloster, S., Magi, B. I., Marlon, J. R., Daniau, A.-L., Field, R. D., Arneth,
1603 A., Forrest, M., Hantson, S., Kehrwald, N. M., Knorr, W., Lasslop, G., Li, F., Mangeon, S., Yue,
1604 C., Kaiser, J. W., & van der Werf, G. R. (2017). Historic global biomass burning emissions for
1605 CMIP6 (BB4CMIP) based on merging satellite observations with proxies and fire models (1750–
1606 2015). *Geoscientific Model Development*, 10(9), 3329–3357. [https://doi.org/10.5194/gmd-10-](https://doi.org/10.5194/gmd-10-3329-2017)
1607 [3329-2017](https://doi.org/10.5194/gmd-10-3329-2017)

1608 Vejnovic, J., Djuric, B., Lombnæs, P., & Singh, B. R. (2018). Concentration of trace and major
1609 elements in natural grasslands of Bosnia and Herzegovina in relation to soil properties and plant
1610 species. *Acta Agriculturae Scandinavica, Section B — Soil & Plant Science*, 68(3), 243–254.
1611 <https://doi.org/10.1080/09064710.2017.1388439>

1612 Voutsas, D., & Samara, C. (2002). Labile and bioaccessible fractions of heavy metals in the
1613 airborne particulate matter from urban and industrial areas. *Atmospheric Environment*, 36(22),
1614 3583-3590.

1615 Wang, Z., Wade, A. M., Richter, D. D., Stapleton, H. M., Kaste, J. M., & Vengosh, A. (2022).
1616 Legacy of anthropogenic lead in urban soils: Co-occurrence with metal(loids) and fallout
1617 radionuclides, isotopic fingerprinting, and in vitro bioaccessibility. *Science of The Total*
1618 *Environment*, 806, 151276. <https://doi.org/10.1016/j.scitotenv.2021.151276>

- 1619 Watson, J. G., Chow, J. C., & Houck, J. E. (2001). PM_{2.5} chemical source profiles for vehicle
1620 exhaust, vegetative burning, geological material, and coal burning in Northwestern Colorado
1621 during 1995. *Chemosphere*, 43(8), 1141–1151. [https://doi.org/10.1016/S0045-6535\(00\)00171-5](https://doi.org/10.1016/S0045-6535(00)00171-5)
- 1622 Webb, N. P., & Pierre, C. (2018). Quantifying Anthropogenic Dust Emissions. *Earth's Future*,
1623 6(2), 286–295. <https://doi.org/10.1002/2017EF000766>
- 1624 Wen, B., Li, L., Duan, Y., Zhang, Y., Shen, J., Xia, M., Wang, Y., Fang, W., & Zhu, X. (2018).
1625 Zn, Ni, Mn, Cr, Pb and Cu in soil-tea ecosystem: The concentrations, spatial relationship and
1626 potential control. *Chemosphere*, 204, 92–100.
1627 <https://doi.org/https://doi.org/10.1016/j.chemosphere.2018.04.026>
- 1628 Whalen, E. D., Smith, R. G., Grandy, A. S., & Frey, S. D. (2018). Manganese limitation as a
1629 mechanism for reduced decomposition in soils under atmospheric nitrogen deposition. *Soil*
1630 *Biology and Biochemistry*, 127, 252–263. <https://doi.org/10.1016/j.soilbio.2018.09.025>
- 1631 Wieder, W.R., Boehnert J., Bonan G. B., & Langseth M. (2014). RegridDED Harmonized World
1632 Soil Database v1.2. Data set. Available on-line [<http://daac.ornl.gov>] from Oak Ridge National
1633 Laboratory Distributed Active Archive Center, Oak Ridge, Tennessee, USA.
1634 <http://dx.doi.org/10.3334/ORNLDAAAC/1247> .
- 1635 Wiedinmyer, C., Lihavainen, H., Mahowald, N., Alastuey, A., Albani, S., Artaxo, P., Bergametti,
1636 G., Batterman, S., Brahney, J., Duce, R., Feng, Y., Buck, C., Ginoux, P., Chen, Y., Guieu, C.,
1637 Cohen, D., Hand, J., Harrison, R., Herut, B., . . . & Zhang, Y. (2018). *COARSEMAP: synthesis of*
1638 *observations and models for coarse-mode aerosols*. AGU Fall Meeting New-Orleans, 2017.
- 1639 Wilcke, W., Krauss, M., & Kobza, J. (2005). Concentrations and forms of heavy metals in
1640 Slovak soils. *Journal of Plant Nutrition and Soil Science*, 168(5), 676–686.
1641 <https://doi.org/10.1002/jpln.200521811>

- 1642 Wong, M. Y., Rathod, S. D., Marino, R., Li, L., Howarth, R. W., Alastuey, A., Alaimo, M. G.,
1643 Barraza, F., Carneiro, M. C., Chellam, S., Chen, Y. C., Cohen, D. D., Connelly, D., Dongarra,
1644 G., Gómez, D., Hand, J., Harrison, R. M., Hopke, P. K., Hueglin, C., ... Mahowald, N. M.
1645 (2021). Anthropogenic Perturbations to the Atmospheric Molybdenum Cycle. *Global*
1646 *Biogeochemical Cycles*, 35(2). <https://doi.org/10.1029/2020GB006787>
- 1647 Woo, D. K., & Seo, Y. (2022). Effects of elevated temperature and abnormal precipitation on
1648 soil carbon and nitrogen dynamics in a *Pinus densiflora* forest. *Frontiers in Forests and Global*
1649 *Change*, 5. <https://doi.org/10.3389/ffgc.2022.1051210>
- 1650 Xianmo, Z., Yushan, L., Xianglin, P., & Shuguang, Z. (1983). Soils of the loess region in China.
1651 *Geoderma*, 29(3), 237–255. [https://doi.org/https://doi.org/10.1016/0016-7061\(83\)90090-3](https://doi.org/https://doi.org/10.1016/0016-7061(83)90090-3)
- 1652 Yalcin, M. G., Battaloglu, R., & Ilhan, S. (2007). Heavy metal sources in sultan marsh and its
1653 neighborhood, kayseri, turkey. *Environmental Geology*, 53(2), 399–415.
1654 <https://doi.org/10.1007/s00254-007-0655-4>
- 1655 Yang, C., Guo, R., Liu, R., Yue, Q., Ren, X., & Wu, Z. (2012). PCA analysis and Concentration
1656 of Heavy Metal in the Soil, Guangdong, China. *Advanced Materials Research*, 518-523, 1952-
1657 1955. <https://doi.org/10.4028/www.scientific.net/AMR.518-523.1952>
- 1658 Yang, S., Zhou, D., Yu, H., Wei, R., & Pan, B. (2013). Distribution and speciation of metals (Cu,
1659 Zn, Cd, and Pb) in agricultural and non-agricultural soils near a stream upriver from the Pearl
1660 River, China. *Environmental Pollution*, 177, 64–70.
1661 <https://doi.org/https://doi.org/10.1016/j.envpol.2013.01.044>
- 1662 Yilmaz, F., Yilmaz, Y. Z., Ergin, M., Erkol, A. Y., Muftuoglu, A. E., & Karakelle, B. (2003).
1663 Heavy metal concentrations in surface soils of Izmit Gulf region, Turkey. *Journal of Trace and*
1664 *Microprobe Techniques*, 21(3), 523–531. <https://doi.org/10.1081/TMA-120023068>

- 1665 Yu, C., Cheng, J. J., Jones, L. G., Wang, Y. Y., Faillace, E., Loureiro, C., & Chia, Y. P. (1993).
1666 *Data collection handbook to support modeling the impacts of radioactive material in soil*. United
1667 States. <https://doi.org/10.2172/10162250>
- 1668 Yu, C., Peng, B., Peltola, P., Tang, X., & Xie, S. (2012). Effect of weathering on abundance and
1669 release of potentially toxic elements in soils developed on Lower Cambrian black shales, P. R.
1670 China. *Environmental Geochemistry and Health*, *34*(3), 375–390.
1671 <https://doi.org/10.1007/s10653-011-9398-y>
- 1672 Yu, H., Chin, M., Yuan, T., Bian, H., Remer, L. A., Prospero, J. M., Omar, A., Winker, D.,
1673 Yang, Y., Zhang, Y., Zhang, Z., & Zhao, C. (2015). The fertilizing role of African dust in the
1674 Amazon rainforest: A first multiyear assessment based on data from Cloud-Aerosol Lidar and
1675 Infrared Pathfinder Satellite Observations. *Geophysical Research Letters*, *42*(6), 1984–1991.
1676 <https://doi.org/10.1002/2015GL063040>
- 1677 Zak, D. R., Freedman, Z. B., Upchurch, R. A., Steffens, M., & Kögel-Knabner, I. (2017).
1678 Anthropogenic N deposition increases soil organic matter accumulation without altering its
1679 biochemical composition. *Global Change Biology*, *23*(2), 933–944.
1680 <https://doi.org/10.1111/gcb.13480>
- 1681 Zender, C. S., Bian, H., & Newman, D. (2003). Mineral Dust Entrainment and Deposition
1682 (DEAD) model: Description and 1990s dust climatology. *Journal of Geophysical Research*
1683 *Atmospheres*, *108*(D14). <https://doi.org/10.1029/2002JD002775>
- 1684 Zhang, H., Wang, S., Hao, J., Wan, L., Jiang, J., Zhang, M., Mestl, H. E. S., Alnes, L. W. H.,
1685 Aunan, K., & Mellouki, A. W. (2012). Chemical and size characterization of particles emitted
1686 from the burning of coal and wood in rural households in Guizhou, China. *Atmospheric*
1687 *Environment*, *51*, 94–99. <https://doi.org/10.1016/j.atmosenv.2012.01.042>

- 1688 Zhang, L., Zheng, Q., Liu, Y., Liu, S., Yu, D., Shi, X., Xing, S., Chen, H., & Fan, X. (2019).
1689 Combined effects of temperature and precipitation on soil organic carbon changes in the uplands
1690 of eastern China. *Geoderma*, 337, 1105–1115.
1691 <https://doi.org/https://doi.org/10.1016/j.geoderma.2018.11.026>
- 1692 Zhang, X.-Y., Tang, L.-S., Zhang, G., & Wu, H.-D. (2009). Heavy Metal Contamination in a
1693 Typical Mining Town of a Minority and Mountain Area, South China. *Bulletin of Environmental*
1694 *Contamination and Toxicology*, 82(1), 31–38. <https://doi.org/10.1007/s00128-008-9569-4>
- 1695 Zhao, B., Zhuang, Q., Shurpali, N., Köster, K., Berninger, F., & Pumpanen, J. (2021a). North
1696 American boreal forests are a large carbon source due to wildfires from 1986 to 2016. *Scientific*
1697 *Reports*, 11(1). <https://doi.org/10.1038/s41598-021-87343-3>
- 1698 Zhao, F., Wu, Y., Hui, J., Sivakumar, B., Meng, X., & Liu, S. (2021b). Projected soil organic
1699 carbon loss in response to climate warming and soil water content in a loess watershed. *Carbon*
1700 *Balance and Management*, 16(1), 24. <https://doi.org/10.1186/s13021-021-00187-2>
- 1701 Zorer, Ö., Ceylan, H., & Doğru, M. (2009). Determination of heavy metals and comparison to
1702 gross radioactivity concentration in soil and sediment samples of the Bendimahi River Basin
1703 (Van, Turkey). *Water, Air, & Soil Pollution*, 196(1–4), 75–87. [https://doi.org/10.1007/s11270-](https://doi.org/10.1007/s11270-008-9758-0)
1704 [008-9758-0](https://doi.org/10.1007/s11270-008-9758-0)